Hochschule Ruhr West

Fachbereich 4 – Institut Mess- und Sensortechnik

Bachelorarbeit

Modeling the hemodynamic effects of a percutaneous deep venous arterialization procedure with subsequent parametric sensitivity analysis

---

Vorgelegt von:

Lennart Koppe
Parkstraße 26
42549 Velbert

Matrikelnummer: 10011368
Fachsemester: 8
Studiengang: Gesundheits- und Medizintechnologien

Abgabe: 02.08.2022

Erstgutachter: Prof. Dr. Carole Leguy
Zweitgutachter: Dr. Ir. Wouter Huberts

Eidesstaatliche Erklärung

Hiermit erkläre ich, dass ich die vorliegende Arbeit eigenständig und ohne fremde Hilfe angefertigt habe. Textpassagen, die wörtlich oder dem Sinn nach auf Publikationen oder Vorträgen anderer Autoren beruhen, sind als solche kenntlich gemacht.

Die Arbeit wurde bisher keiner anderen Prüfungsbehörde vorgelegt und auch noch nicht veröffentlicht.

Velbert, 02.08.2022

Ort, Datum

Unterschrift

Abstract

People with Chronic Limb Ischemia (CLI) suffer from severely blocked arterial vessels in the leg and foot. Due to insufficient blood circulation, rest pain, ulcers, gangrene, and infections occur in the ischemic foot region. Patients in whom classic countermeasures such as bypass and angioplasty fail are referred to as no-option patients. Normally the only treatment option left for this group of patients is a major amputation. Since this disease is expected to become more frequent in the future due to the increasing incidence of diabetes mellitus and an aging society, more research is needed on alternative methods. One of these is the relatively new percutaneous deep venous arterialization procedure (pDVA). A method whose aim is to bring pressurized blood to the ischemic tissue via the venous system. This is achieved with the help of stents and the destruction of a venous valves. Results to date have been very satisfactory, although cure rates can vary widely. Currently, the exact hemodynamic changes caused by the procedure are poorly understood. Therefore, this work attempts to recreate in silico the vasculature in the foot, mimic blockages caused by CLI, and finally simulate and study the effects of the pDVA procedure. This is done using an open-loop model. The pressure curves and flow volumes in the foot could only be simulated and interpreted to a limited extent. The main reason for this is the current lack of data on the geometric and mechanical properties of the foot vessels. Nevertheless, it was found that the great saphenous vein, venous lateral perforators in the midfoot region, the posterior tibial artery, the lateral plantar vein, and the 1st metatarsal deep vein could be of great importance for the outcome of the procedure. Thus, these vessels might need special attention for modeling the procedure or answer the question of feasibility. However, the results can only be taken with caution. Future work must strive to improve available data for modeling hemodynamics in the vessels of the foot. In addition, it is believed that the use of a closed-loop model with more complex venous valves would lead to better results.

Contents

1 Introduction 1
1.1 Peripheral arterial disease 1
1.2 Critical limb ischemia 1
1.3 Vascular system in the leg and foot 2
1.3.1 Overview 2
1.3.2 Arteries - leg 2
1.3.3 Arteries - foot 3
1.3.4 Veins - foot 3
1.3.5 Veins - leg 5
1.4 Symptoms of CLI 5
1.4.1 Pain 5
1.4.2 Ulcer and gangrene 5
1.4.3 Quality of life (QoL) 6
1.4.4 Mortality 6
1.5 Current treatment options for CLI 6
1.5.1 Overall strategy 6
1.5.2 Drug treatment 6
1.5.3 Amputation 6
1.5.4 Bypass and Angioplasty 7
1.5.5 Venous arterialization 7
1.5.6 Superficial Venous Arterialization (SVA) 8
1.5.7 Deep Venous Arterialization (DVA) 8
1.5.8 Percutaneous DVA (pDVA) with the LimFLow system 8
2 Aim and Thesis Outline 10
3 Methods 11
3.1 Overview 11
3.2 Pulse Wave Propagation Model 11
3.2.1 Vascular network 11
3.2.2 Geometrical and mechanical data 13
3.2.3 Cardiac output signal 14
3.3 0D model 14
3.3.1 Resistance 15
3.3.2 Compliance 16
3.3.3 Inertance 16
3.4 Artery-Vein-Connections 17

3.5 Venous valves 18
3.6 Windkessel model 18
3.7 pDVA implementation 19
3.8 Boundary Conditions and Assumptions 20
3.9 Numerical implementation 20
3.10 Sensitivity Analysis 22
3.10.1 Motivation 22
3.10.2 Implementation 22
4 Results 24
4.1 Verification of the Model 24
4.1.1 General characteristics of the healthy vascular system 24
4.1.2 Flow distribution in the foot 26
4.1.3 Blood pressure in the foot 28
4.2 Sensitivity analysis 30
5 Discussion 31
5.1 Summary and interpretation 31
5.2 Limitations 32
5.3 Future studies 33
6 References 34
7 Appendix 38

1 Introduction

1.1 Peripheral arterial disease

The peripheral arterial disease (PAD) is a slowly progressive narrowing of the arterial vessels especially in the legs due to fat deposits and calcification. The result of this is reduced blood supply to the lower limbs that can cause intermittent claudication, also known as symptomatic PAD. These patients experience lower limb pain during exercise, which is alleviated after a 10-minute rest.[2,3] Risk factors are similar to those of coronary artery disease and cerebrovascular disease. Diabetes, cigarette smoking, age, and hypertension have the highest correlations with the occurrence of PAD.[4] Studies have shown that PAD can be found in 15-20% of the population in the United States older than 70 years.[5,6]

1.2 Critical limb ischemia

The end-stage of PAD is called critical limb ischemia (CLI). This group of patients affected by CLI is classified in the Rutherford Scale 4-6 and the Fontaine classification 3-4. In this case, the lower leg arteries are largely occluded.[7,8] This has the consequence that the blood circulation of the lower limb, especially in the foot, is greatly disturbed. This condition usually worsens gradually up to the most severe form of CLI which is called "desert foot" because of very poor blood circulation. Symptoms are rest pain, ulcers, and/or gangrene in the foot due to the persistent lack of oxygenated blood.[7] For Europe and North America approximately 500 - 1000 new CLI cases per year in a population of 1 million are expected.[2] Due to the increasing global trend of diabetes and an aging population, it can be assumed that the rate of CLI patients will continue to grow in the future because of the correlations of Diabetes and Age with the occurrence of PAD.[4,9–11]

Rutherford stage	Fontaine stage	Description/definition
0	I	Asymptomatic
1	IIa	Mild claudication
2	IIb	Moderate claudication
3	IIb	Severe claudication
4	III	Rest pain
5	IV	Ischemic ulcers of the digits of the foot (minor tissue loss)
6	IV	Severe ischemic ulcers of the digits of the foot (major tissue loss)

Figure 1, Rutherford-Becker and Fontaine classification in PAD[12]

1.3 Vascular system in the leg and foot

1.3.1 Overview

This work examines the hemodynamic effects of a percutaneous deep venous arterialization in a patient with CLI. A disease that affects the vascular system, especially in the leg and foot. For that reason, an overview of the relevant vessels is first given. Arteries and veins together form two circulatory systems: The systemic and pulmonary blood circulation. In the systemic circulation, blood travels from the aorta to arteries throughout the body. In the distal direction, they divide into smaller vessels. Arteries with a diameter smaller than 100 µm are called arterioles and those with a diameter of 5-10 µm are called capillaries. It is at the capillaries that oxygen finally diffuses into the surrounding tissue where it is used for metabolic processes. In addition, carbon dioxide is absorbed there and transported back to the heart. Latter is done by the venous system. In the proximal direction, veins become larger as more and more of these join. After the venous blood has reached the heart, it is reoxygenated through the pulmonary circulation and thus the blood circulation in the body is complete.

1.3.2 Arteries - leg

Note that the vascular network variabilities in the foot are not discussed in this work. Instead, the vascular system of the lower limbs is generalized and thus simplified. We start at the aorta in the abdomen. Two arterial branches, each for one leg, arise from it: The common iliac arteries. The common iliac artery gives off a branch (internal iliac artery) to supply the pelvic viscera[*]. The other part passes through the inguinal ligament[†] and becomes the femoral artery. Subsequently, the femoral artery gives off a branch (profunda femoris) to supply the thigh. The other part continues to the knee joint where it becomes the popliteal artery. The popliteal artery divides into two tibial arteries: The anterior and posterior tibial artery. The anterior tibial artery provides perforators for the anterior aspect of the leg and in the ankle region, it becomes the dorsalis pedis which supplies the upper aspect of the foot (dorsal side). The posterior tibial artery supplies the posterior aspect of the leg and ends in the lower part of the foot (plantar side). Shortly after the branching from the popliteal artery, another branch emerges from a posterior tibial artery, which runs along the lateral part of the calf. This so-called peroneal or fibular artery ends in the calcaneal part of the foot.[13,14]

[*] Collective term for bladder, rectum, pelvic genital organs and terminal part of the urethra

[†] A band running from the pubic tubercle to the anterior superior iliac spine

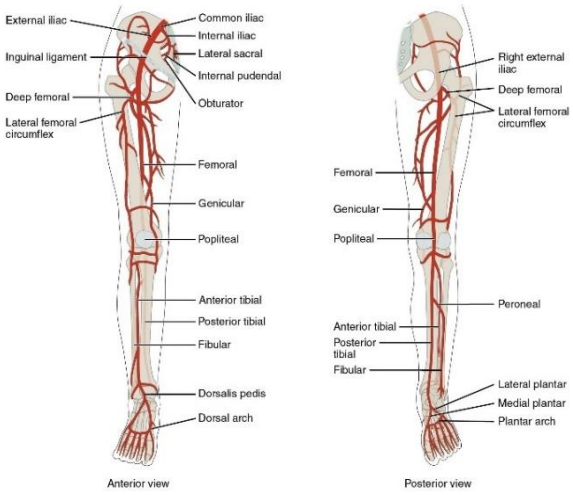

Figure 2, Arterial Network of the leg[15]

1.3.3 Arteries - foot

The dorsal and plantar networks in the foot are very similar. In both sides, an arch is formed that extends across the lateral and medial regions of the foot and rejoins proximally to the toes, where it gives off metatarsal arteries. These supply the toes with blood. In addition, there are some perforators on the metatarsal side that connect the dorsal aspect with the plantar aspect of the foot.[16–18]

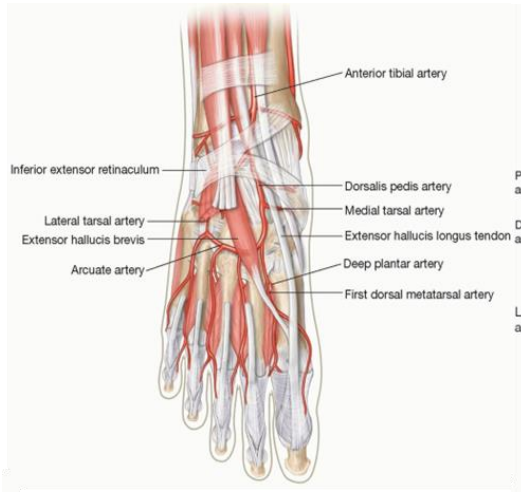

Figure 3, Dorsal side of foot arteries[19]

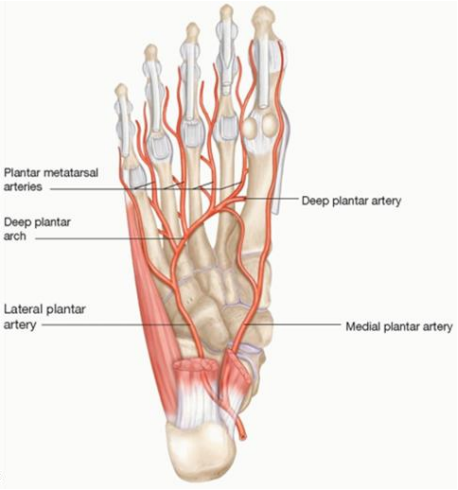

Figure 4, Plantar side of foot arteries[19]

1.3.4 Veins - foot

The venous system in the lower foot can be divided into three categories: In the foot, there are the **deep and superficial veins**. The deep veins are located under the deep fascia‡ of the foot and run along the large arteries. The superficial veins are in the tissue of the subcutis until they eventually drain into the deep veins. **Perforators** connect the superficial veins with the deep system. The deep veins of the plantar side are:

‡ Tissue which sorrounds muscels

1. Deep plantar venous arch: This is the counterpart of the arcuate artery (see Figure 3). It runs along with the first to the fifth metatarsal and receives metatarsal veins that drain the blood from the toes. It is often found doubled.
2. Medial plantar vein: This arises from the deep plantar venous arch and runs along the medial aspect of the foot. It receives blood from surrounding muscles and tissues.
3. Lateral plantar vein: This is a continuation of the lateral end of the deep plantar venous arch. It runs along the lateral part of the foot until it joins the medial plantar vein which forms the posterior tibial vein. Both, the medial and lateral plantar veins are often doubled.

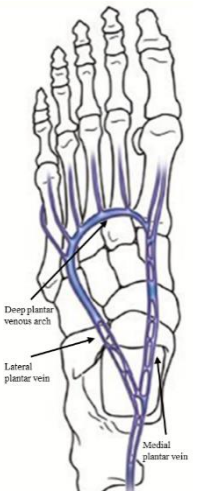

Figure 5, The Plantar side of foot veins[1]

In addition, there is the counterpart to the peroneal artery: The peroneal vein. This takes blood from the calcaneal part of the foot. Besides the deep veins in the plantar side, there are many small superficial veins on the sole. When the foot is stepped on, these act like a sponge that is squeezed out and fill surrounding veins with blood.[20] The superficial veins of the dorsal side are:

1. The dorsal arch: It lies over the proximal ends of the metatarsal bones and receives blood from the dorsal metatarsal veins.
2. The medial marginal vein originates from the medial side of the dorsal arch and runs across the medial side until it becomes the Great Saphenous Vein (GSV).
3. The lateral marginal that arises on the lateral side of the dorsal arch. This runs along the lateral side of the dorsal foot and ends in the Small Saphenous Vein (SSV).

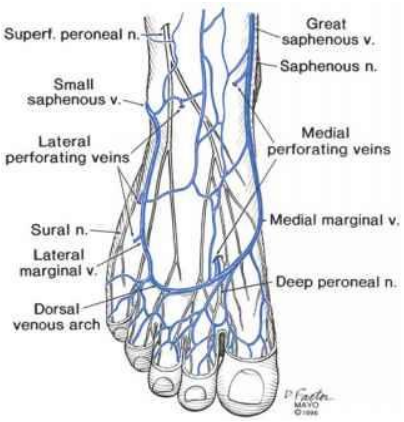

Figure 6, The dorsal side of foot veins[24]

Additionally, perforators connect the GSV, the SSV, and the anterior tibial vein with the plantar aspect of the foot.[21,22] This can be seen in Figure 7.

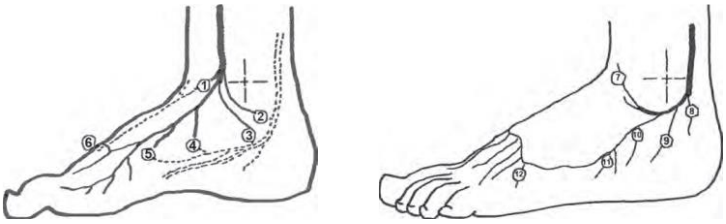

Figure 7, Left: Perforators at the medial side that connect the GSV with deep plantar veins, Right: Perforators at the lateral side that connect the SSV with the deep plantar veins. Numbers indicate where the perforators penetrate the deep facscia.[22]

1.3.5 Veins - leg

The GSV runs medially to the thigh to perforate the deep fascia. It joins the common femoral vein around the hip. The SSV ascends behind the lateral malleolus[§] to join the popliteal vein. The tibial veins and the peroneal vein are connected just like the associated arteries. The posterior tibial vein runs along the posterior part and the anterior tibial vein runs along the anterior aspect of the lower leg. Together they form a popliteal vein, which continues towards the hip. In the hip area, continuations of the popliteal, deep femoral, and the great saphenous vein come together and end up the inferior vena cava.[20,23]

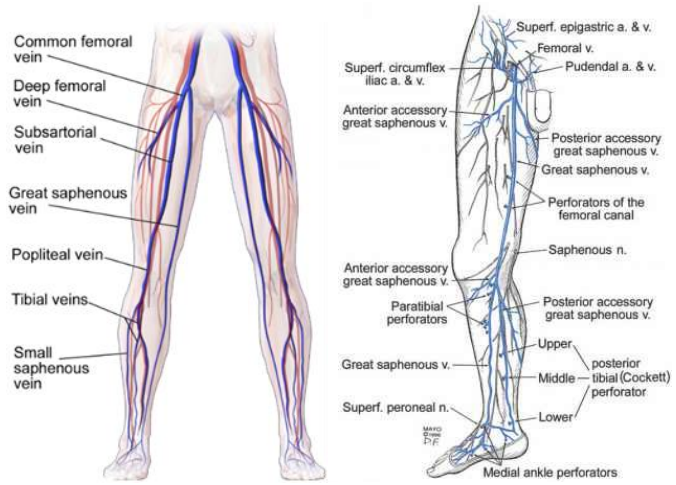

Figure 8, Veins of the leg[24,25]

1.4 Symptoms of CLI

1.4.1 Pain

The pain occurs mainly in the foot. It is caused by ischemia, tissue loss, ischemic neuropathy, or a combination of these. The pain is often described as excruciating and, unlike attenuated PAD, it can even occur at rest. Typically, the pain takes place at night, which causes the patient to have greatly reduced sleep. In addition, walking is nearly impossible.[2]

1.4.2 Ulcer and gangrene

Gangrene represents a decomposition of the tissue. It occurs primarily on the toes but may also be found on the heel in bedridden patients. In severe cases, the decomposition goes from the toes to the midfoot.[2] Ulcer is defined as necrosis and rupture of superficial tissue layers. It can be found on the toes and reaches the bones in some cases. Both ulcers and gangrene are caused by minor traumas. Exemplary are local pressure points (e.g. ill-fitting shoes).[26] Normally, these wounds would heal in a healthy patient. However, due to insufficient perfusion, the healing process is greatly slowed. This can

[§] A bone protrusion located on the lateral side at the distal end of the calf bone

lead to the wounds not healing and the condition of these even worsening. There is also an increased risk of infection at the ischemic tissue.

1.4.3 Quality of life (QoL)

There is an extremely poor outlook for diagnosed CLI patients. QoL is severely deteriorated in these people. Sprengers et al.[27] have shown that QoL is lower in CLI patients than in patients with chronic kidney disease, chronic heart disease, or cancer. This was found out with the so-called SF-36 questionnaire. A widely accepted, reliable, and commonly used tool to assess QoL.

1.4.4 Mortality

Also, the life expectancy after diagnosis is dramatically shortened. After one year, approximately 25% of the patients have died and another 25% have undergone major amputations. After five years, less than 50% are alive.[2,27,28] These high rates of death and amputation show that current treatment options are limited and that CLI continues to be a challenge.

1.5 Current treatment options for CLI

1.5.1 Overall strategy

CLI is a complex macro- and microvascular disease where the body responds with increasing angiogenesis, capillary sprouting, and expansion of preexisting collaterals to counteract the lack of blood circulation in the foot. These natural countermeasures often fail and therefore medical and surgical therapies must be performed when CLI is diagnosed.[7,8] In addition to wound care, there are several treatment approaches for CLI patients to reduce risk factors and symptoms, prevent major amputation, improve quality of life and increase survival.[29] To achieve these goals, most CLI patients must undergo revascularization in addition to medication. For patients with other severe co-morbidities or for those in whom revascularization has a poor chance of success, amputation may be the most appropriate treatment.[2]

1.5.2 Drug treatment

All CLI patients receive drug treatment. For example, vasodilators to dilate the vessels or drugs to counteract metabolic abnormalities due to PAD are used. The goal is to reduce symptoms of claudication and to avoid events related to atherosclerosis (myocardial infarction, stroke, or death). Unfortunately, this approach does not lead to a significant reduction or elimination of symptoms.[2]

1.5.3 Amputation

In the case of amputations, a distinction must be made between minor and major amputations. Minor amputations involve amputations below the ankle (toe, metatarsal, or forefoot) and major amputations involve amputations above the ankle.

Minor amputations may be part of a limb salvage strategy. Combined with revascularization of the limb the ambulatory status and the quality of life can be preserved. Amputations above the ankle may be necessary when the patient's life is in danger due to systemic infections, severe pain at rest cannot be reduced, failed revascularizations, or when necrotic processes in the foot have progressed too far.[2,30] Major limb amputations are a very big break in the lives of the affected patients. On the one hand, the quality of life deteriorates significantly and, on the other hand, life expectancy drops sharply after a major amputation.[31,32] Therefore, a major amputation is the last choice of all treatment options and is generally attempted to be avoided. Many major amputations can be prevented through successfully performed revascularization and therefore this will be discussed in more detail next.[2]

1.5.4 Bypass and Angioplasty

Both bypass surgery and angioplasty have their restrictions. Whether one of the methods can be used depends on many different physiological factors: anatomical lesions, distribution of arterial disease, patient's health status, comorbidities, presence of foot ulcer, foot infection, and local expertise.[33]

In many cases, bypass operation is an effective way to avoid major limb amputation. But this technique has its limitations and therefore it is not feasible for every CLI patient, especially for those with severe comorbidities. If there are for example severe occlusions below the ankle, no vessels could provide perfusion to the distal foot after bypass surgery. This is the case in 14-18% of all CLI cases. Especially patients with additional diabetes tend to have more distal occlusions and therefore it can be assumed that the ratio of people where the bypass surgery is not feasible will increase because of the global trend of diabetes.[11]

Angioplasty seems to be more tolerant in patients with comorbidities. Also, it can be performed gradually in several steps on fragile patients or be repeated in case of an unsuccessful procedure. However, this method also has its limitations in feasibility and is therefore not as promising as bypass surgery in some cases.[33]

People, for whom bypass surgery and angioplasty are not applicable or for whom these interventions have failed, are often referred to as "no-option" patients. The last chance for these people to avoid a major limb amputation and/or to relieve rest pain is called venous arterialization.[34]

1.5.5 Venous arterialization

CLI mainly affects arterial vessels. Conversely, the venous system is largely free of occlusions in some CLI cases. This fact is exploited in the venous arterialization procedure. The idea is that after the procedure, arterial outflow to the ischemic tissue should be ensured through part of the disease-free venous system so that the capillaries can be retrogradely filled with blood. This is achieved by placing a connection between an artery and a vein proximal to the arterial blockage. In addition to this fistula, the distal venous valves must be destroyed, as they only allow blood flow in the direction to the heart. After the procedure blood flow and pressure in the foot increase drastically. It must be remembered

that due to the procedure the body lacks a complete vein in the foot to drain the blood. Due to reverse venous flow in the following days, there is a high risk of swelling, pain, and superficial necrosis at the foot which subsides after a while.[35]

Venous arterialization is indeed a serious intervention on the patient's body that drastically changes the hemodynamics. Nevertheless, a meta-analysis from 2006 by Lu et al.[36] found that, on average, the limb salvage rate of venous arterialization after one year is 71%. There are various approaches to implement this concept of vascular remodeling. Simplified, there are two main methods, which are the superficial and deep venous arterialization.

1.5.6 Superficial Venous Arterialization (SVA)

In the SVA procedure, a connection is made between the Great Saphenous Vein (GSV) and an appropriate artery (usually the popliteal artery). Thus, through the superficial veins on the dorsal side, the arterial flow to the foot is created. From the medial marginal vein to the fistula, the valves are destroyed by a so-called valvulotome. In addition, side branches of the superficial venous arch, which would lead to direct arterial backflow to the heart, are ligated to prevent subsequent shunting and to increase the antegrade perfusion pressure.[11,34]

1.5.7 Deep Venous Arterialization (DVA)

Unlike the SVA procedure, the DVA procedure uses the deep venous arch for arterial outflow. Often the posterior tibial artery and one of the concomitant veins are used. Less commonly, concomitants of the dorsal pedal artery are used. According to van den Heuvel et al.[34], there are two advantages in the DVA over SVA:

- The deep venous system is not dependent on the superficial veins to get sufficient perfusion of the foot.
- In the DVA procedure, fewer venous valves need to be destroyed compared to SVA.

Both, SVA and DVA can be performed by surgical or percutaneous approach. Usually, the percutaneous approach is preferred because it creates smaller wounds in the very slowly healing ischemic tissue and reduces the risk of infection. In addition, a surgical approach seems to be more difficult to perform.[34] Since this work focuses on the percutaneous DVA procedure, this type of venous arterialization will be examined in more detail.

1.5.8 Percutaneous DVA (pDVA) with the LimFLow system

The LimFlow system (LimFlow SA, Paris, France) is currently the only one that makes the DVA procedure possible percutaneously. In the following, the pDVA procedure with the LimFlow system is described.

Two catheters need to be placed into the patient. One is inserted on the arterial side through a femoral sheath. Inside this hollow catheter, there is a needle connected to a guidewire. On the venous side, a

sheath is made by puncturing the posterior tibial vein near the ankle and a second catheter is inserted. Both catheter tips are moved to the planned crossing point. The catheters are then aligned so that the needle of the catheter in the artery can penetrate the arterial and venous wall. With the help of the catheter in the vein, the needle is then grasped and pulled in the distal direction to the foot. The cable is then replaced with a thicker cable and a valvulotome is connected to its end. It is a cutting basket that is designed in such a way that the hooks inside make the venous valves incompetent and at the same time protect the vessel wall. This valvulotome is pushed from the crossing point to the midfoot so that all the venous valves in between become useless. After pre-dilation of the vessels, 5.5mm stents are stacked from the ankle to the crossing point. These ensure sufficient caliber of the vessels and complete destruction of the venous valves. In addition, the stents are covered so that no venous cross-connections (collaterals) can steal blood. The fistula and pDVA procedure are completed with the help of a special stent that connects the vein and artery. Proximally the caliber is 3.5mm and distally 5.5mm. The reason is to bridge the different diameters between both vessels. This stent is also covered to prevent blood leakage.[37]

2 Aim and Thesis Outline

Despite great success of the percutaneous DVA method, it does not provide equal improvement in every patient. Limb salvage rates are high and yet wound healing rates vary. Also, reinterventions must be performed frequently. Important for a successful procedure is to get enough pressurized blood to the distal foot.[38–40] The aim of this work is to improve the understanding of the hemodynamic effects of the pDVA procedure and to highlight which vessels need special intention then modeling this intervention or to answer the question of feasibility.

To do so, a general 0D-open-loop model with emphasis on the pedal vessels is presented that mimics the hemodynamics in the human body. In addition, a parameter sensitivity analysis is performed. The analysis is used to investigate the impact of certain vessels on the outcome of the procedure. This is important because the number of measurements performed by the physician is limited. Therefore, the analysis might help to define a measurement protocol and to develop patient-specific models.[41]

First, information is given how the model was created and how the associated sensitivity analysis was performed. Specifically, the network of all vessels, its data, assumptions, numerical implementation and the type of sensitivity analysis is described. After creating the model for a healthy human, it is checked to what extent it mimics the physical properties of the real human vascular system. Finally, the results of the simulated percutaneous deep venous arterialization procedure are discussed.

3 Methods

3.1 Overview

To obtain a realistic picture of the effects of the pDVA procedure, all major arterial and venous vessels of the human body are implemented in the numerical model. These vessels and the associated artery-vein-connections (lumped model for peripheral vessels) consist of concatenated 0D models. This was done for all vessels above the ankle using the global multiscale model of Müller and Toro[42]. The information for the vascular network and the geometrical and mechanical properties of each vessel are taken from that work. Since the cerebral area is elaborated very detailed there, it is simplified. In addition, to investigate the effects of the pDVA procedure in the foot, numerous small vessels below the ankle are added. Their network and associated parameters were estimated using various studies. It should be noted that this is an open-loop model (unlike the model of Müller and Toro). This means that the venous return at the superior and inferior vena cava drains through a Windkessel model in each case. Therefore, there is no type of feedback for the cardiac output and so the cardiac output signal is the same for each period.

3.2 Pulse Wave Propagation Model

3.2.1 Vascular network

In the model, the vascular system is divided into segments. Each of the segments is assigned a different reference number. All used segments and their corresponding reference are shown in Figure 9 - Figure 12. Blue dots in the arterial network and red dots in the venous network display a simple link of two or more vessels while a yellow diode symbol represents a venous valve between segments. Green dots indicate a connection of the arterial and venous system by peripheral vessels. There are additionally outlined the simplification of the cerebral area and the extended vascular representation of the foot. Note that the segment with number 98 (Vertebral venous plexus) is removed.

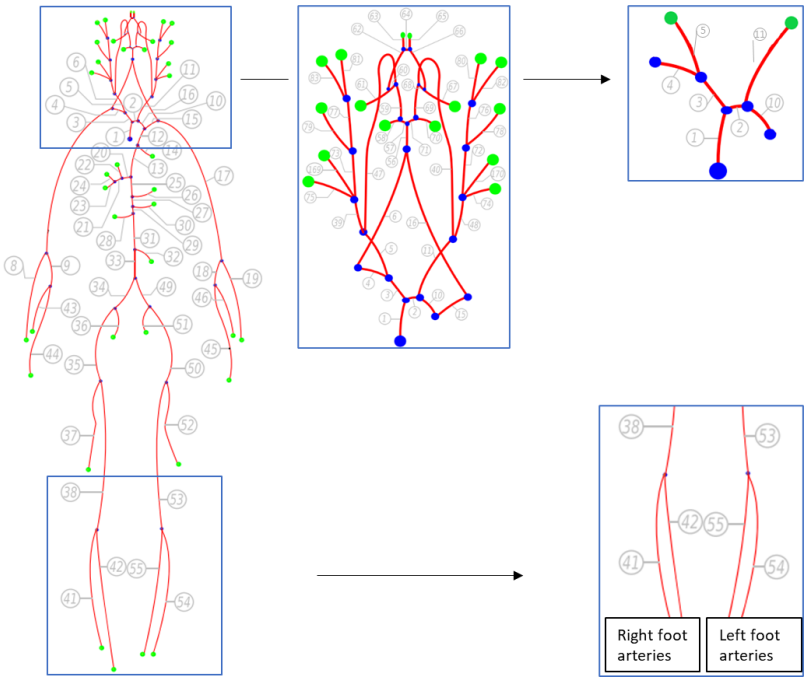

Figure 9, Arterial network after Müller and Toro[42] (modified)

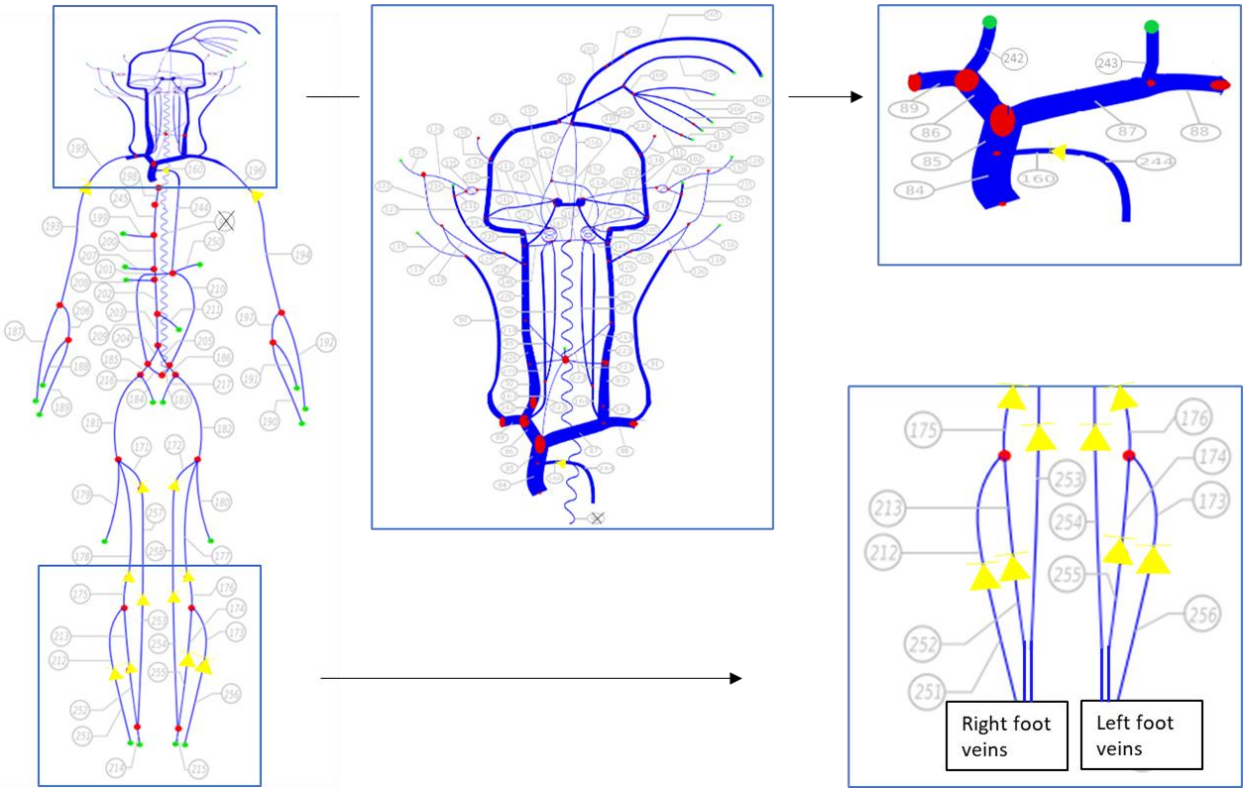

Figure 10, Venous network after Müller and Toro[42] (modified)

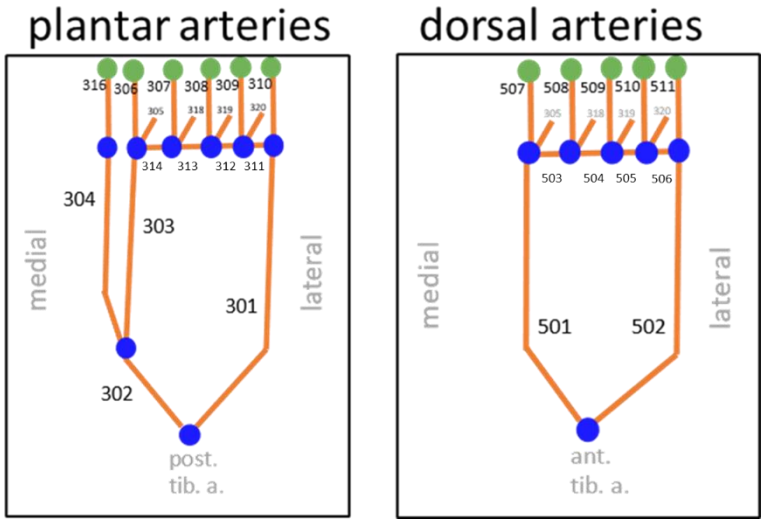

Figure 11, Arteries in the right foot with references. Note that the references in the left foot correspond to those of the right foot, increased by 100.

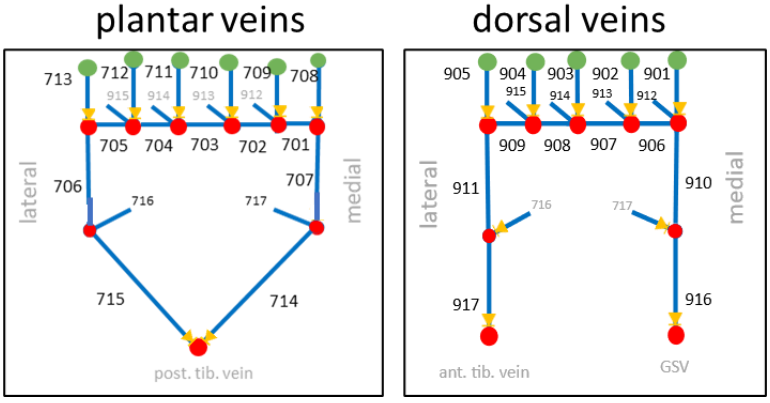

Figure 12, Veins in the right foot with references. Note that the references in the left foot correspond to those of the right foot, increased by 100.

3.2.2 Geometrical and mechanical data

To define the segments in the numerical model three values of each vessel section are needed: The length of the vessel *l*, the inner radius *r*, and the wave speed *c*. In Appendix A Table 4 shows all geometric and mechanical values used for the model, which were taken from the work of Müller and Toro. Table 5 and Table 6 show the remaining values of the pedal area. In literature, data of pedal vessels are scarce. For that reason, missing values were estimated. Missing geometrical and mechanical data of the pedal vascular system is estimated by several approaches. It is assumed that the wave velocity in the arterial and venous system of the foot does not change significantly. With this assumption, wave velocities in the foot were estimated using available data from nearby tibial vessels. Missing data of radii was estimated by Murray's law[43] or by nearby geometrical ratios. Murray's Law can be seen in (1), where r_m is the radius of the mother vessel and r_i is a branching daughter vessel. The geometrical ratios are taken from literature and nearby vessels.

$$r_m{}^3 = r_1{}^3 + r_2{}^3 + (\dots) + r_n{}^3 \qquad (1)$$

Since the arterial and venous networks are very similar, it is also assumed that an artery and its associated vein are of the same length. Thus, missing vessel lengths were estimated by the associated vessels of the arterial/venous system.

No geometric data was found about the venous perforators in the midfoot (see Figure 7). Two vessels were implemented to summarize the network of these in the foot (segment 716 and 717 in Figure 12). Their diameter are arbitrarily set to be 3 mm.

3.2.3 Cardiac output signal

The input signal for the system is intended to mimic the blood ejection of a human heart. It is a modified signal from the work of Olufsen et al.[44] and can be seen in Figure 13. The cardiac cycle there has a period of 1 second, and its mean flow is 5.38 $\frac{l}{min}$. One cardiac cycle consists of 201 data points.

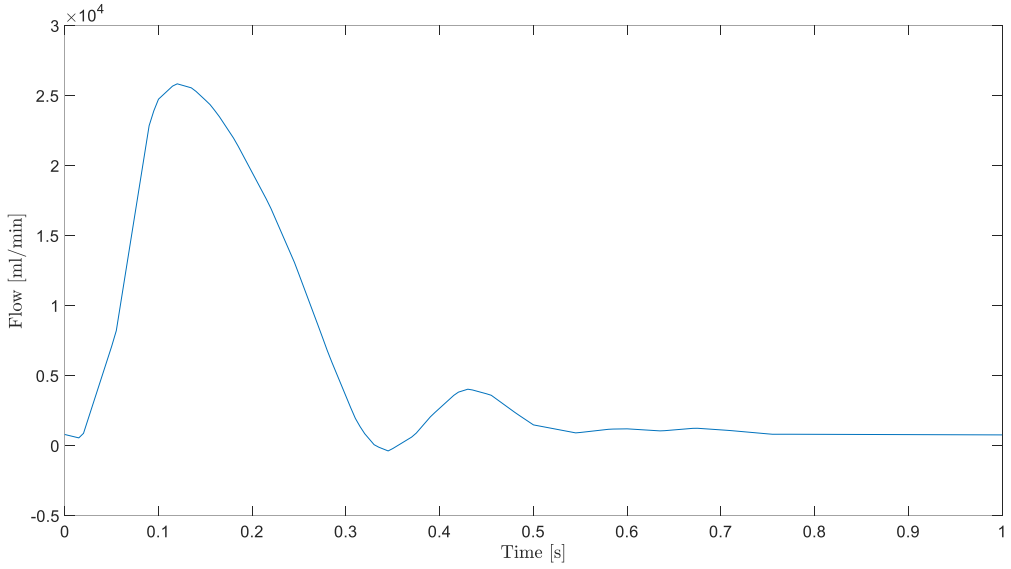

Figure 13, Cardiac output signal with mean flow rate of 5.38 $\frac{l}{min}$ and period of 1s

3.3 0D model

Each of the segments is implemented using a 0D model with three different elements. In the electrical analogy, the 0D model consists of a resistor connected in series with a coil. The coil represents the inertia of the blood. Before and after these two elements, a capacitor is connected, which imitates the storage capacity of the vessel (see Figure 14). Since two capacitors are included, storage capacity is halved in each case. All three elements (*C*, *R*, and *L*) must be quantified for each vessel segment. The equations for the elements are presented below.

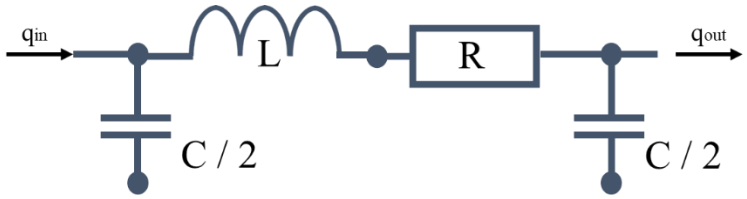

Figure 14, 0D model representation for vessel segments. C: Compliance, R: Resistance, L: Inertance, q: Flow

Table 1, Constants

Symbol	Value	Unit	Description
$\boldsymbol{\eta}$	0,0045	$Pa \cdot s$	Blood viscosity
$\boldsymbol{\rho}$	1050	$\frac{kg}{m^3}$	Blood density
$\boldsymbol{\tau}$	1,5	s	Time constant

3.3.1 Resistance

In the following, most of the equations are based on the book "Snapshots of Hemodynamics" from Westerhof et al.[45] The resistance *R* is the ratio between blood pressure and flow (2). Thus, the higher the resistance, the greater is the pressure drop along a vessel segment for the same blood flow.

$$R = \frac{\Delta p_R}{q_R} \qquad (2)$$

The resistance of each vessel is calculated with Poiseuille's law. The flow velocity v_r along the radius *r* can be described using equation (3) with the pressure gradient Δp_R over a tube with length *l* and the radius of the tube r_i. The velocity profile is characterized by a parabolic shape where the maximum velocity is in the center of the tube.

$$v_r = \frac{\Delta p_R \cdot \left(r_i^2 - r^2\right)}{4 \cdot \eta \cdot l} \qquad (3)$$

The average velocity v_{mean} over that parabolic profile is derived from (3) and given by equation (4).

$$v_{mean} = \frac{\Delta p_R \cdot r_i^2}{8 \cdot \eta \cdot l} \qquad (4)$$

The relationship between velocity *v* and volumetric flow *q* along a tube is as follows:

$$v = \frac{q}{\pi \cdot r_i^2}. \qquad (5)$$

Combining (5) and (4) we obtain equation (6). It defines the mean flow in the tube.

$$q_R = \frac{\Delta p_R \cdot \pi \cdot r_i^4}{8 \cdot \eta \cdot l} \qquad (6)$$

After reshaping equation (6) according to the form in (2) the result is the Poiseuille resistance of a tube (7) where A is the cross-sectional area.

$$R = \frac{8 \cdot \eta \cdot l}{\pi \cdot r_i^4} = \frac{8 \cdot \eta \cdot l \cdot \pi}{A^2} \qquad (7)$$

3.3.2 Compliance

The compliance C of a vessel describes how much the volume V of the tube changes with the distending pressure Δp_C:

$$C = \frac{\Delta V}{\Delta p_C}. \qquad (8)$$

In the time domain, the relationship between the blood flow q_C and the transmural pressure p_C is described by the proportionality constant C (9).

$$q_C = C \cdot \frac{\partial p_C}{\partial t} \qquad (9)$$

For the calculation of C, a derivative of the Moens-Korteweg equation is used. The Moens-Korteweg equation establishes a relationship between wave speed c and the incremental elastic modulus E_{inc} for non-viscous fluids (10) where h is the wall thickness.

$$c = \sqrt{\frac{h \cdot E_{inc}}{2 \cdot r_i \cdot \rho}} \qquad (10)$$

A derivative of the Moens-Korteweg equation described by Bramwell and Hill[46] among others gives a relation between wave speed and the area compliance C_A (11). The area compliance is defined in (12) where l is the length of the vessel.

$$c = \sqrt{\frac{A}{\rho \cdot C_A}} \qquad (11)$$

$$C_A = \frac{C}{l} \qquad (12)$$

After (12) is inserted in (11) and converted to C we get the final equation for calculating the compliance in each vessel (13).

$$C = \frac{l \cdot A}{\rho \cdot c^2} \qquad (13)$$

3.3.3 Inertance

The inertance is the effective mass of the blood. It is defined as follows:

$$L = \frac{\rho \cdot l}{A}. \qquad (14)$$

Newton's second law (15) states that a heavier mass m accelerates slower than a lighter mass under the same force F. This also applies to blood in the human body.

$$F = m \cdot \frac{\partial v}{\partial t} \qquad (15)$$

The force that leads to an acceleration of the blood in a vessel can be formulated by the pressure difference along the tube times the cross-sectional area (16).

$$F = \Delta p_L \cdot A \qquad (16)$$

The mass of the blood is equal to the density times the volume of a tube, thus

$$m = \rho \cdot V = \rho \cdot A \cdot l. \qquad (17)$$

Substituting (16) and (17) into Newton's second law and considering the relationship between flow and velocity from equation (5), we obtain (18). Hence, the inertance is a proportionality factor that brings together the oscillation of the blood pressure and the acceleration of the blood.

$$\Delta p_L = L \cdot \frac{\partial q_L}{\partial t} \qquad (18)$$

3.4 Artery-Vein-Connections

The connections between the arterial and venous system (AV-connections) summarize all smaller vessels whose network can no longer be accurately described. The behavior of these many small vessels can nevertheless be mimicked. This is realized by a network of 0D models already presented above. In the model, most of the AV-connections are a series of an input impedance and 0D models which are taken from Müller and Toro[42]. One exception is present in the celiac area. There the AV-connection is more complex. Since, the cerebral region is simplified and the pedal region is expanded, the values for the AV-connections there are adjusted.

To avoid non-physiological reflections, an input impedance Z_{inp} is connected in series before each AV-connection. This is recommended according to Alastruey et al.[47] The formula calculating the impedance is taken from Matick[48] and can be seen in (19) where L_{term} and C_{term} are the C-L-values and Z_{term} is the characteristic impedance of the terminal arterial segment.

$$Z_{inp} = Z_{term} = \sqrt{\frac{L_{term}}{C_{term}}} \qquad (19)$$

In order not to change the total peripheral resistance of the AV connection R_{per}, the resistance in the 0D model is calculated as in (20), so that the sum of the AV resistance R_{AV} and Z_{inp} equals R_{per}, which is defined as the mean pressure drop divided by the mean blood flow across the peripheral vessels.

$$R_{AV} = R_{per} - Z_{inp} \qquad (20)$$

All values of the AV-connections in the model can be seen in Appendix B. Each AV-connection above the ancle consists of three 0D models (arteriolar, capillary, and venular part) and the input impedance attached in front of it (see Figure 15). Additionally, the more complex AV-connection at the celiac artery can be seen in Figure 16. There, four of the capillary 0D models join before the

venule part. The terminal arteries in the foot are each connected to the corresponding veins. For this purpose, the values for the AV-connections in the ankle region from the work of Müller and Toro were combined into one 0D model and adjusted (see Table 9).

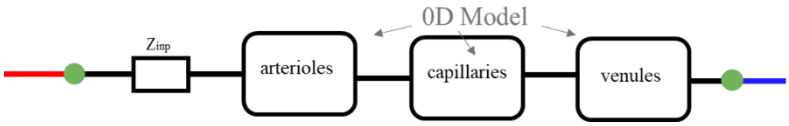

Figure 15, Network of a simple artery-vein-connection after Müller and Toro[42]. Red vessel represents the arterial part and blue vessel the venous part. The corresponding values are in Table 7.

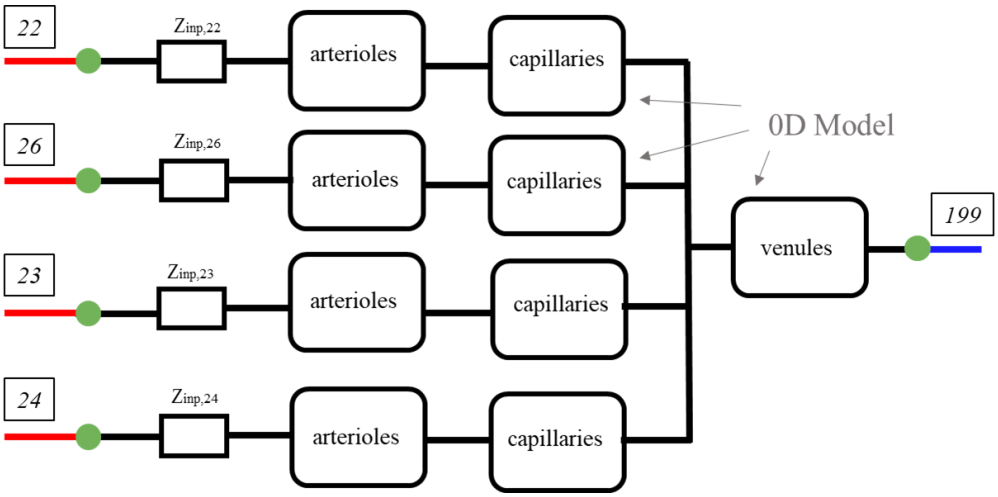

Figure 16, Network of complex artery-vein-connection after Müller and Toro[42]. The corresponding values are in Table 8.

3.5 Venous valves

Venous valves are implemented as ideal diodes. Thus, when the pressure gradient across the segment does not correspond to the desired flow direction, the resistance is increased to mimic valve closure. The flap closes instantaneously in the model with an increase of the resistance by a factor of 10^{21}.

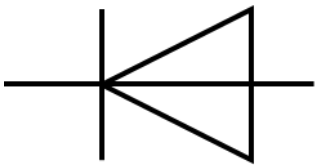

3.6 Windkessel model

The inferior and superior vena cava are the terminal vessels of the venous system that carry all blood back to the heart. In the human body this venous backflow is subsequently reoxygenated by the pulmonary circulation and returned to the arterial system. Since this is an open-loop model, the blood flow in the model is not returned to the system but drains through a three-element Windkessel model (see Figure 17). First, the total peripheral resistance and compliance for the Windkessel models are

determined. After that, the input impedance Z_{inp} and the resistance R are calculated in the same way as described for the AV-connections, see (19) and (20).

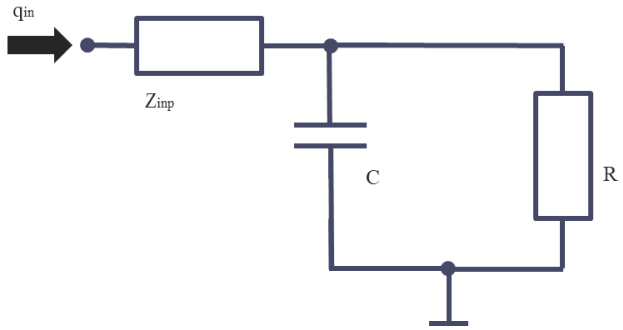

Figure 17, Windkessel-model with Z_{inp}: input impedance, R: resistance and C: compliance.

For the determination of the peripheral resistance, the mean pressure, and the mean flow rate in the caval vein are required. The mean return rate for the superior vena cava is estimated to be 30% of cardiac output.[49] The remaining blood volume is returning through the inferior vena cava. The central venous pressure (pressure in caval veins) is estimated to be 6 mmHg.

The relationship of R and C in a RC link can be described by the time constant τ in (21). It shows how much time is needed for the initial pressure over R to drop by 37%.[45] The constant τ is set to 1,5 seconds.[50] After inserting (20) in (21), we get the final equation to calculate C (22). All values for the two Windkessel models can be found in Table 2.

$$\tau = R \cdot C \qquad (21)$$

$$C = \frac{\tau}{(R_{per} - Z_{inp})} \qquad (22)$$

Table 2, Values for the Windkessel models. Units are C $[\frac{ml}{mmHg}]$ and $R_{per}|Z_{inp}$ $[\frac{mmHg \cdot s}{ml}]$.

Vessel	Z_{inp}	Rper	C
Superior vena cava	0,05	0,22	8,44
Inferior vena cava	0,05	0,10	34,87

3.7 pDVA implementation

Before implementing the pDVA procedure, the diameters of the arteries in the lower limbs were first greatly reduced to resemble the physiology of a CLI patient. Thereupon, a connection between the posterior tibial artery and vein in the right leg (segment nr. 41 and 251) is mimicked by a crossing stent. The length of the stent is 4 cm, and its proximal diameter is 3,5 mm while the distal diameter is 5,5 mm. It is implemented as a 0D model analogous to all other vessels. In addition, all venous valves between crossing-point and mid-foot are removed. Finally, the diameter of the tibial vein is increased

to 5 mm due to the covered stents. See Figure 18, which outlines the implementation of the pDVA procedure.

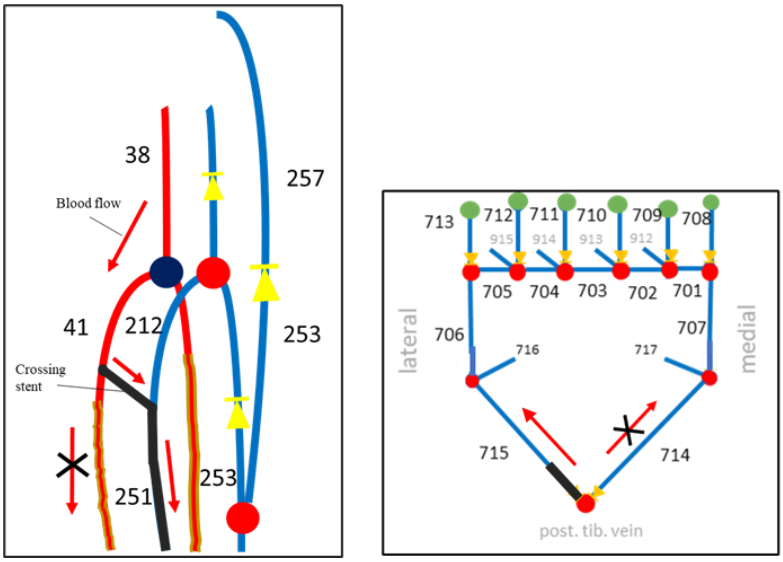

Figure 18, pDVA implementation, where crossing stent connects the post. tibial artery with post. tibial vein. Yellow diode symbols indicate implemented valves. Note that direct flow from posterior tibial vein to the medial plantar aspect of the foot is cut off due to the covered stent.

3.8 Boundary Conditions and Assumptions

Pressure: The initial pressure of each vessel segment is set to 0 mmHg.

Flow: It is assumed that the blood flow in the vascular system is steady and laminar. All vessels have the shape of a uniform tube. This must be assumed to apply Poiseuille's law (3) and Murray's law (1).

CLI pathophysiology: The reduction in diameter due to occlusions is assumed to be 50%.[51]

Crossing stent: It is assumed that the crossing stent has no significant compliance. Thus, the compliance there is set to 0 ml/mmHg.

System filling: Since all vessels are empty in the first cycle, the system must be filled before it can be interpreted meaningfully. After 16 cardiac cycles, it is assumed that the system is filled and has stabilized. The simulation starts with no initial flows.

3.9 Numerical implementation

The model is implemented using the software MATLAB R2019a (MathWorks, Natick, MA, USA). The presented segments are partitioned to a maximum length of 10 cm by linear interpolation. Each of the elements in the 0D model (resistance, inertia, and compliance) is discretized by two nodes that can take to values: pressure and flow. Thus, two degrees of freedom are present in every node. Interconnected segments share nodes to provide continuity. In the following, the discretization of the 0D model elements (Figure 19) and the creation of the system of equations according to Kroon et al.[52] are presented.

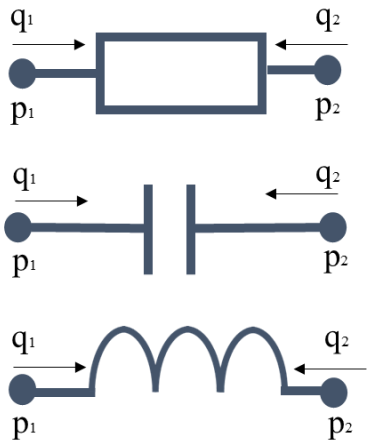

Figure 19, Discretization of the 0D model where q is the blood flow and p is the pressure. Note that the flow directions are directed inwards.

In (2), (9), and (18) all three element equations are already described, which give the relationship between pressure and flow:

$$q_R = \frac{1}{R} \cdot \Delta p_R, q_C = C \cdot \frac{\partial p_C}{\partial t}, and\ \Delta p_L = L \cdot \frac{\partial q_L}{\partial t}. \qquad (23)$$

Considering the discretization in Figure 19, the equations from (23) can be formulated in matrices as

$$\frac{1}{R} M \begin{pmatrix} p_1 \\ p_2 \end{pmatrix} = \begin{pmatrix} q_1 \\ q_2 \end{pmatrix}, \qquad (24)$$

$$CM \begin{pmatrix} \frac{\partial p_1}{\partial t} \\ \frac{\partial p_2}{\partial t} \end{pmatrix} = \begin{pmatrix} q_1 \\ q_2 \end{pmatrix}, \text{ and} \qquad (25)$$

$$\frac{1}{L} M \begin{pmatrix} \int p_1\, dt \\ \int p_2\, dt \end{pmatrix} = \begin{pmatrix} q_1 \\ q_2 \end{pmatrix} \qquad (26)$$

with

$$M = \begin{pmatrix} 1 & -1 \\ -1 & 1 \end{pmatrix}. \qquad (27)$$

Assembling the equations (24), (25), and (26) leads to

$$R_e p_e + C_e \frac{\partial p_e}{\partial t} + L_e \int p_e\, dt = q_e\ , \qquad (28)$$

where p_e and q_e are are the nodal point pressures and flows. C_e contains the compliances while R_e and L_e contain the inverse values for the resistances/ impedances and inertias. The values after a time step Δt are calculated by the first order backwards scheme and the first order trapezium rule. The resulting system of equations is

$$K_e p_e^{t+\Delta t} = f_e q_e^{t+\Delta t}, \qquad (29)$$

with the system matrix K_e defined as

$$K_e = \frac{3}{2\Delta t} C_e + R_e + \frac{\Delta t}{2} L_e \qquad (30)$$

and the right-hand side

$$f_e = -C_e \left(-\frac{2}{\Delta t} p_e^t + p_e^{t-\Delta t} \right) - L_e \frac{\Delta t}{2} p_e^t. \quad (31)$$

Note that the system matrix K_e is constant. Since the flow of each element is directed inwards, $q^{t+\Delta t}$ is zero for all nodes except those with prescribed external flow. Thus, the system of equations can be solved.

3.10 Sensitivity Analysis

3.10.1 Motivation

The set of input data for the model is referred to as *Z*. Each of its elements z_1, z_2, …, z_n is estimated by physiological data from measurements and assumptions with their accompanying simplifications. Due to limited measurement precision, simplifications, and biological parameters changing over time, the parameters z_i are afflicted with an error. Each of these inaccuracies contribute to the total error of the output *Y*. The purpose of a sensitivity analysis is to identify the parameters that are relevant for *Y* and its error. Thus, it is hoped that the analysis highlights which parameters must be paid special attention to when modeling the pDVA procedure. Since the model is computationally expensive, a local sensitivity analysis is performed. It determines the local impact of input factor varieties.

3.10.2 Implementation

The local sensitivity analysis is defined as the partial derivative of the output Y.[53] See (32)

$$S = \frac{\partial Y}{\partial z_i}, \qquad (32)$$

where *S* is the set of sensitivity indices. Due to the high computation time, this idea of analysis is simplified. Therefore, only the local impact of diameter varieties on flow is examined. This is done by calculating the local standard deviation of the volume flow of all preselected vessels by diameter changes. In addition, every single absolute standard deviation has been calculated in relation to the sum of all absolute standard deviations.

The standard deviation σ with the Bessel's correction is defined as

$$\sigma_{y^{(z)}} = \sqrt{\frac{1}{N-1} \sum_{i=1}^{N} (y_i^{(z)} - \overline{y^{(z)}})^2} \qquad (33)$$

with the number of samples per segment *N* and the mean of these samples $\overline{y^{(z)}}$ where *z* stands for the observed segment.

Since theoretically any diameter of the vessels is possible, but not equally likely, the input space must be well chosen. In the paper from Khan et al.[54] the average relative standard deviation of the diameter of the dorsalis pedis artery is about 0.3. If a normal distribution is assumed for the occurrence of the diameters, then the interval $\mu \pm 0.5\mu$ contains more than 90% of the total set, where μ is the expected value for the radius. The resulting interval is adopted for all remaining vessels. A total of 5 equally distributed samples in each interval are used for the sensitivity analysis ($N = 5$).

4 Results

4.1 Verification of the Model

4.1.1 General characteristics of the healthy vascular system

We will now see if the model mimics the physiology of a healthy human vascular system. Listed below are some characteristics of the blood pressure in an average healthy human described by the book “Snapshots of Hemodynamics” by Westerhof et al.[45]

(1) The average mean pressure in the aorta is about 100 mmHg.
(2) The mean pressure in the foot is only a few mmHg lower compared to the aorta.
(3) The venous resistance is about $\frac{1}{20}$ of the total resistance. Thus, the central venous pressure is about 5 mmHg, assuming that the mean aortic pressure is 100 mmHg.
(4) Pressure waves in the peripheral arteries present:
    a. amplification of the systolic pressure amplitudes
    b. smoothing of the pulse
    c. time delay
    d. secondary reflection in the diastolic part of the wave

(1) The mean pressure of around 100 mmHg in the aorta and (2) the slight pressure drop to the foot can be clearly seen in Figure 22. (3) The central venous pressure appears to be around 5 mmHg. (4) Although an amplification of the systolic amplitudes can be seen in Figure 20 they appear to be very small. The smoothing of the pulse is not present. The pulses in peripheral vessels show secondary reflections and are delayed.

Figure 21 compares calculated non-pathological mean volumetric flows with measurements from literature. Most values included there are within the measurement ranges. Only the blood flow in the iliac artery seems to be too low.

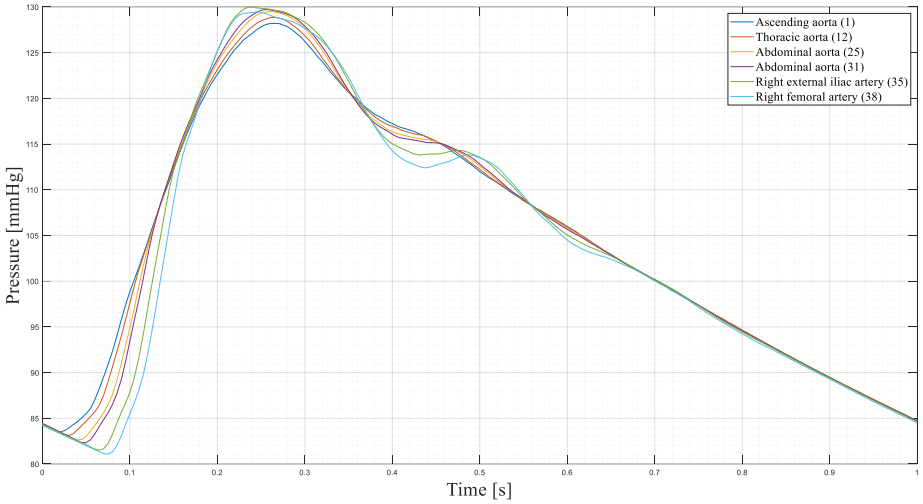

Figure 20, Calculated pressure curves of a healthy human from the Aorta to the legs. Numbers in the legend are the reference numbers from Table 4.

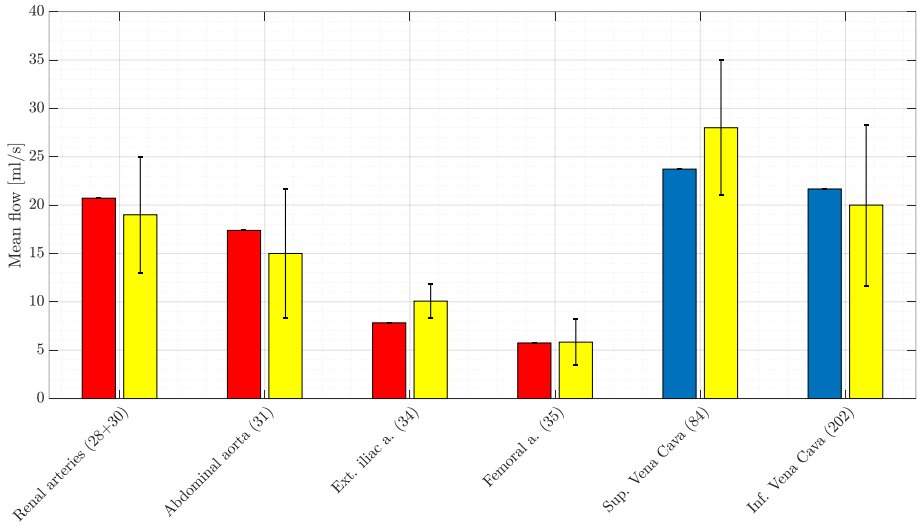

Figure 21, Calculated mean flows in arteries and veins for a healthy human. Numbers at the bar labels are the reference numbers from Table 4. Yellow bars show measurements from literature.[55–59]

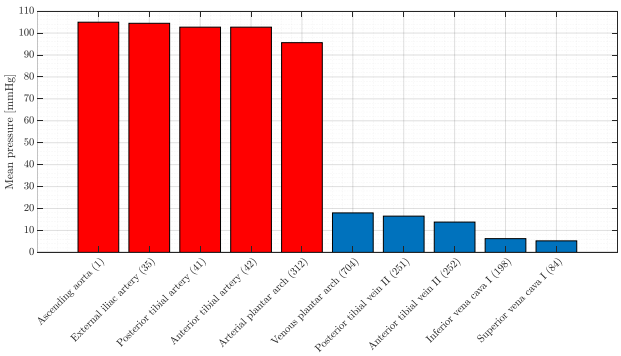

Figure 22, Calculated mean pressure values in arteries and veins for a healthy human. Numbers at the bar labels are the reference numbers from Table 4.

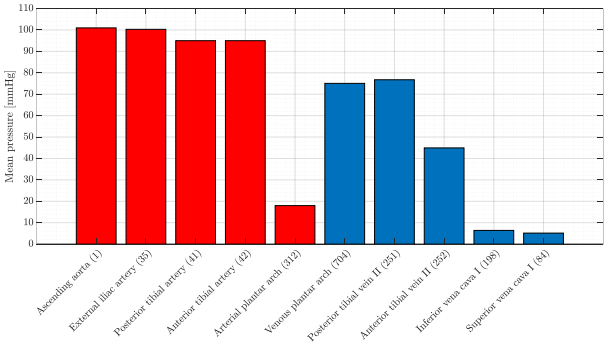

Figure 23, Calculated mean pressure values in arteries and veins for a CLI patient after pDVA procedure. Numbers at the bar labels are the reference numbers from Table 4.

4.1.2 Flow distribution in the foot

Non-pathological arteries

Figure 24, Figure 25, and Figure 26 show the calculated distributions of the mean blood flows in the lower limb for a healthy, CLI, and post-pDVA patient. In the implemented healthy arterial system 52% of the blood from the femoral artery goes into the dorsal aspect of the foot (ca. 70 ml/min) and 48% into the plantar aspect (ca. 65 ml/min). In the dorsal side of the foot the blood flow is divided almost equally between medial and lateral arteries which does not agree with measurements of Liang.[60] He measured around 12 ml/min blood flow through the dorsalis pedis artery. In the plantar side the blood flows mainly laterally. That is because no blood flows through the deep branch of the medial arch (segment 303). In addition, no blood flow is noted through the arterial perforators.

Non-pathological veins

The situation is different in the implemented venous part of the foot. There, a small blood circulation through the perforators in the toe area can be found. Overall, the volume flow there is much more evenly distributed among the vessels compared to the pedal arteries. The blood drains most equally divided between the posterior tibial, anterior tibial and great saphenous vein back to the heart.

CLI

Figure 24, Figure 25, and Figure 26 clearly show that the implementation of the stenoses lead to a sharp decrease of blood circulation in the foot. In total, about 20 ml/min of blood reach the pedal vessels there.

pDVA

In the simulated post-pDVA patient blood is directed from the posterior tibial artery to the posterior tibial vein through the crossing stent and eventually reaches the deep venous system in the foot. There, similar to a short circuit, a considerable part of the blood is transported through the lateral perforator to the dorsal aspect of the foot and finally back to the heart via the GSV and anterior tibial vein. Nevertheless, approximately 165 ml/min of blood reaches the plantar arch. Half of this volume flows to the superficial veins through the 1st metatarsal perforator. The rest is transported to the superficial system via the medial perforator. Note that blood flow from the posterior tibial vein is cut off directly to the medial aspect of the foot by the implemented covered stents.

As a benchmark for a successful pDVA procedure, the volume flow in the crossing stent is considered. A volume flow of more than **364 ml/min** indicates a successful procedure while a volume flow of less than **195 ml/min** indicates a failed procedure.[61] In the model presented here, this flow rate after procedure is around **460 ml/min** (see Figure 24).

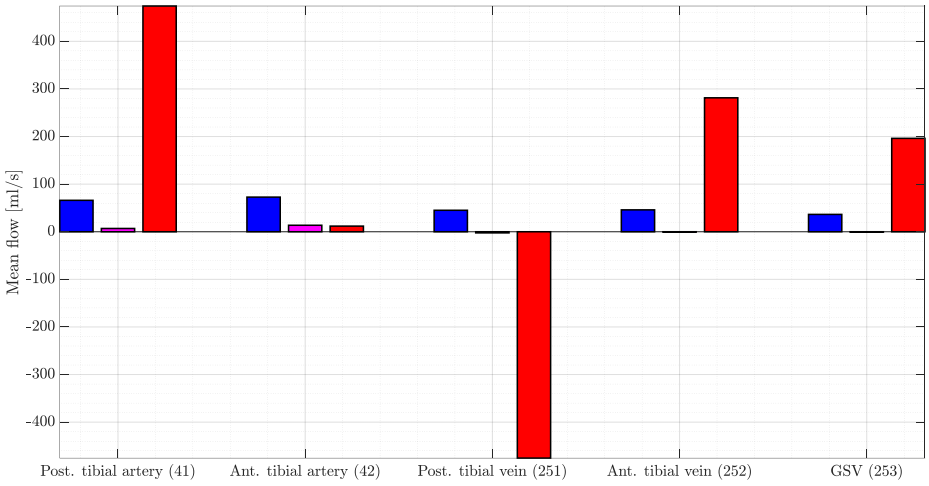

Figure 24, Calculated mean flows for healthy (blue), CLI (pink) and post-pDVA (red) patient in main arteries and veins for the foot. Negative flow indicates that flow direction is reversed due to the pDVA procedure.

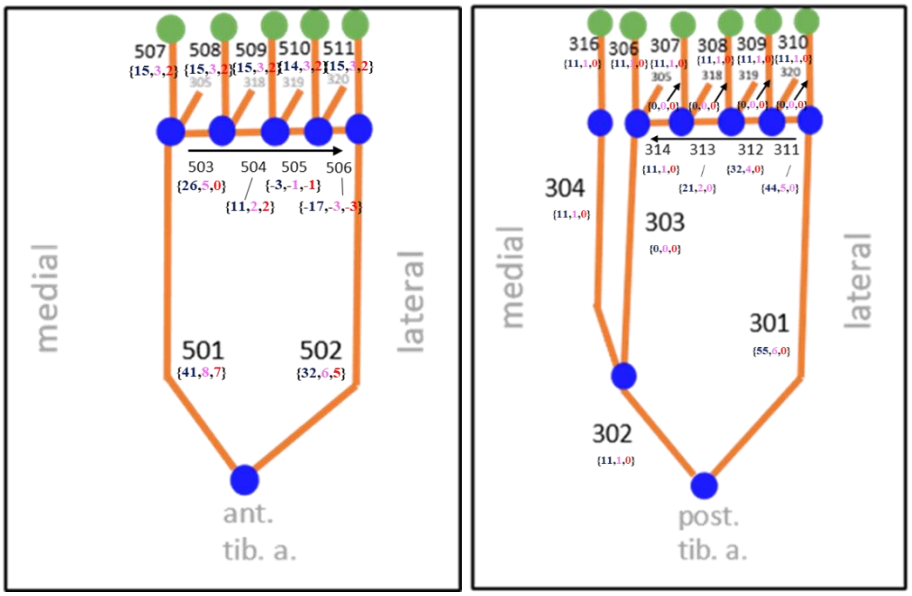

Figure 25, *Calculated mean flows for healthy (blue), CLI (pink) and post-pDVA (red) patient in arterial system of the foot. Colouring for the three cases is taken from Figure 24. Arrows indicate flow direction. All flow values are given in [ml/min].*

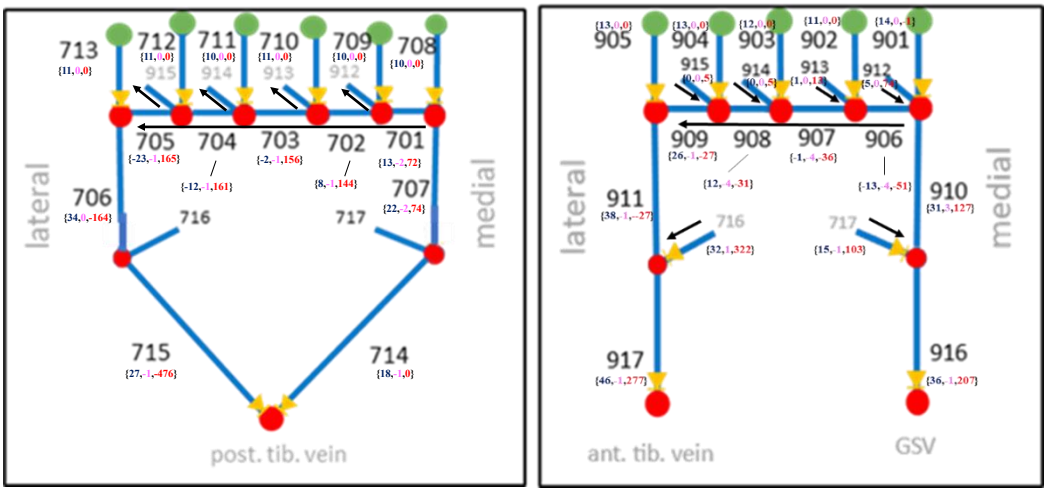

Figure 26, Calculated mean flows for healthy (blue), CLI (pink) and post-pDVA (red) patient in venous system of the foot. Colouring for the three cases is taken from Figure 24. Arrows indicate flow direction. All flow values are given in [ml/min].

4.1.3 Blood pressure in the foot

Non-pathological arteries

Figure 27 and Figure 28 show the calculated pressure curves and a measurement of Bollinger et al.[62] in the posterior tibial artery. Both curves have a period of one second. While the pressure curve from literature lies in the range of 65 to 150 mmHg, the range for the calculated signal is located between 80 and 130 mmHg. In addition, the calculated signal appears to have a significantly higher diastolic pressure. This suggests that the compliance of the surrounding vessels may have been overestimated in the model. Figure 27 and Figure 29 show the calculated pressure curves in non-pathological foot arteries. It is noticeable that the shapes of the pressure curves along the vessels in the foot do not change. Only the offset decreases and delay increases the more distally the curve is measured.

Non-pathological veins

Figure 30 gives an example of the calculated pressure curves in the veins of the foot for a healthy subject. The curve fluctuates very strongly and therefore it cannot be interpreted in a meaningful way.

pDVA

As expected, blood pressure in the foot veins increased sharply after the pDVA procedure (compare Figure 22 and Figure 23). In addition, pressure in the observed arteries is decreased for the post-pDVA patient.

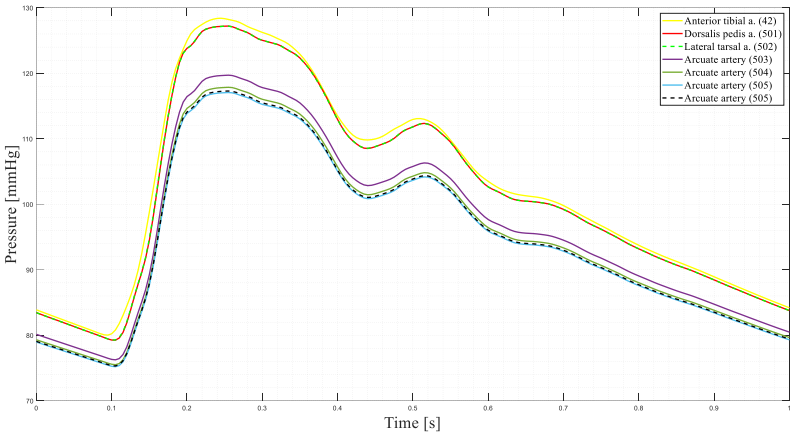

Figure 27, Calculated pressure waves in dorsal arteries of foot in healthy subject.

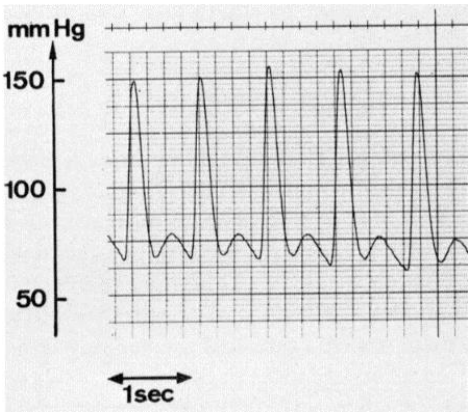

Figure 28, Recorded pressure waves in posterior tibial artery by Bollinger et al.[1]

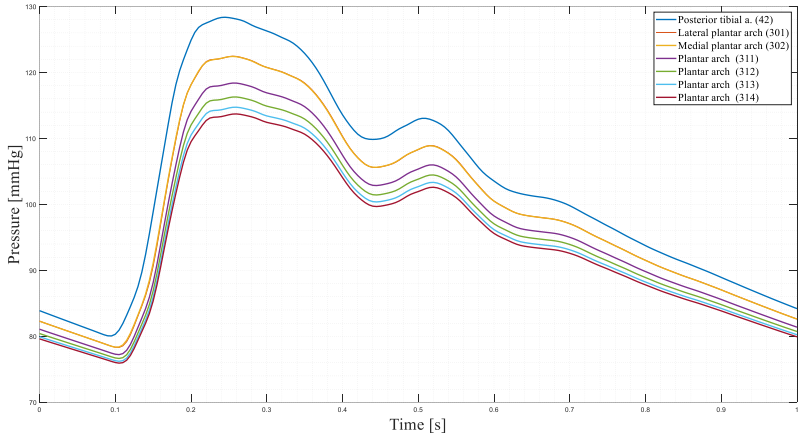

Figure 29, Calculated pressure waves in plantar arteries of foot in healthy subject.

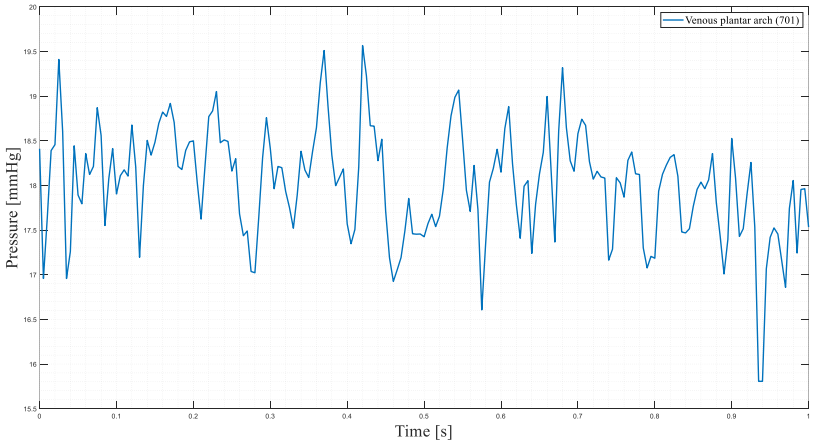

Figure 30, Exemplary pressure curve in the foot veins.

4.2 Sensitivity analysis

The result of the sensitivity analysis (Table 3) is that the largest variances due to locally varying diameters are in the great saphenous vein, the implemented venous lateral perforator in the midfoot region, the posterior tibial artery, and the 1st metatarsal deep vein. Thus, diameter changes of these four vessels have locally the strongest influence on blood flow. A change in the diameters of the anterior tibial artery and the medial plantar vein have the least effect on flow volume locally. The lateral tarsal vein (segment 911) has the highest relative variance.

Table 3, Calculated local flow variances for pre-selected vessels. Standard deviations $\sigma_{y^{(z)}}$ of the calculated volume flows are given in [ml/min].

Vessel	$\sigma_{y^{(z)}}$	$\frac{\sigma_{y^{(z)}}}{\overline{y^{(z)}}}$	$\frac{\sigma_{y^{(z)}}}{\sum \sigma_{y^{(z)}}}$
Great saphenous vein (253)	154,61	0,740	0,161
Lateral perforator (716)	109,67	0,444	0,114
Posterior tibial artery (41)	98,97	0,238	0,103
1. Deep plantar vein (912)	75,69	0,867	0,079
Plantar arch (704)	44,81	0,259	0,047
Plantar arch (703)	44,50	0,264	0,046
Plantar arch (705)	44,49	0,250	0,046
Medial perforator (717)	43,55	0,534	0,045
Lateral plantar vein (715)	43,24	0,096	0,045
Plantar arch (702)	42,25	0,271	0,044
Posterior tibial vein (251)	37,37	0,084	0,039
Medial plantar vein (707)	28,20	0,321	0,029
Plantar arch (701)	27,92	0,312	0,029
Lateral tarsal vein (911)	24,50	1,532	0,025
Lateral tarsal vein (917)	23,17	0,093	0,024
Dorsal vein of the great toe (916)	18,98	0,088	0,020
Dorsal vein of the great toe (910)	15,89	0,130	0,017
2. Deep plantar vein (913)	14,34	0,885	0,015
Dorsal venous arch (909)	12,98	0,961	0,013
Dorsal venous arch (908)	11,72	0,649	0,012
Dorsal venous arch (907)	10,71	0,481	0,011
Lateral plantar vein (706)	10,60	0,065	0,011
Dorsal venous arch (906)	10,56	0,288	0,011
4. Deep plantar vein (915)	5,99	0,939	0,006
3. Deep plantar vein (914)	5,46	0,911	0,006
Anterior tibial artery (42)	1,34	0,120	0,001
Medial plantar vein (714)	0,00	1.158	0,000

5 Discussion

5.1 Summary and interpretation

In summary, calculated blood pressures and blood flows in the main arteries and veins appear to be physiological in many aspects. Nevertheless, the implemented vessels in the foot are not yet all optimally calibrated. Especially the foot arteries present volume flows that certainly do not correspond to reality. Flow rates of 0 ml/min through some arteries can be found. This suggests that some spatial ratios between vessels in the foot are incorrect. In addition, the pressure curve of the posterior tibial artery, does not seem to be reasonable compared with literature. It is assumed that the compliances of the foot vessels are overestimated.

The overall blood return in the foot veins is more equally distributed among the vessels. Also, the uniformly distributed return over the posterior tibial, anterior tibial and great saphenous vein is in accordance with the expectations, because all three veins have the same diameters, which may be an indicator for similarly large flow volumes. However, the pressure curves in the foot veins are not interpretable and not physiological. It is believed that the instantaneous closing of the ideal venous valves is responsible for this but does not have a significant impact on the mean blood flows.

The outcome of the sensitivity analysis suggests that the diameters of the great saphenous vein, the venous lateral perforators in the midfoot region, the posterior tibial artery, the lateral plantar vein, and the 1st metatarsal deep vein need to be evaluated for modeling or planning the pDVA procedure. This is in partial agreement with Migliara.[35] He notes that the 1st metatarsal deep vein perforator is the most important vessel when evaluating perforators for a pDVA procedure. It is noticeable that vessels with a large diameter have a bigger effect on local blood flow than vessels with a small diameter. This makes sense if we assume that a higher diameter indicates a higher average blood flow. Poiseuille's law (6) says that a change in diameter leads to a change of the vessel's resistance. The resistance corresponds to the ratio of the pressure drop over the vessel and the average blood flow through the vessel. Assuming that the pressure drop does not change significantly, a doubling of the diameter leads to an increase of the average blood flow by a factor of 16. It therefore makes a difference in the sensitivity analysis how much blood goes through the vessels on average.

The lowest sensitivity results are also justifiable. The varied diameter sizes of the anterior tibial artery and the medial plantar vein have no impact on the local blood flow. This is in accordance with expectations because only small blood flows are assumed in either vessel. For the anterior tibial artery, the stenoses are to blame and for the medial plantar vein the covered stent does not allow direct blood flow from the posterior tibial vein to the medial part of the deep venous system.

The high relative variance of the lateral tarsal vein (segment 911) can be explained by the fact that there is a potential short-circuit connection in the form of a perforator proximal to the segment. In the electrical analogy, this is speaking about two parallel resistors. An increase in resistance 1 leads to more flow through resistance 2. In other words, the proximal perforator in the model compensates the increase in the resistance of the lateral tarsal vein and vice versa. Since the goal of the pDVA procedure is to have as much pressurized blood flow as possible to the toes, the ratio of the diameters of these two vessels may be of significant importance to the physician. But it must be remembered that the lateral perforator (segment 716) substitutes several parallel perforators (compare Figure 7 and Figure 12).

5.2 Limitations

This model presented here is an 0D-open-loop model. So, there is no feedback on pressure and flow changes in the body. Such feedback could be especially important in a pDVA procedure, which strongly changes the hemodynamics in the body.

The model shows that the results are only partially physiological. Calculated flow volumes and pressure curves above the ankle appear to be realistic. The results below the ankle should be considered with caution. Geometric and mechanical data for vessels in the foot have been found deficient in literature, whereupon many estimates had to be made there. It is believed that the scarce data for foot vessels in literature is currently the biggest problem when modeling hemodynamic effects in the foot.

During the verification of the model, characteristics below the ancle were noticed which are not physiological. These are untypical flow volumes and pressure curves in the non-pathological vessels. The model is currently not able to generate realistic pressure curves in the vessels of the foot. For at least the arterial part, it is assumed that the compliances of the vessels there were estimated too high. The strongly alternating pressure curves in the foot veins are probably caused by the venous valves, which have been implemented as ideal diodes.

Overall, the crossing stent was implemented in a simplified manner. On the one hand, the importance of the site of the crossing stent and its geometrical properties were not investigated. On the other hand, it was assumed that the crossing stent has simplified no compliance. The latter is certainly not correct.

In addition, it should be kept in mind that the local sensitivity analysis was performed in a very simplified way due to time constraints. Only the local impact on blood flow by diameter variances was studied. Thus, the mutual influence of parameters and their global impact was not investigated.

5.3 Future studies

It is strongly recommended that future work strive to create a better data set regarding the geometric and mechanical data of the vessels in the foot. Better data would certainly provide more realistic results. In addition to the geometrical and mechanical properties, however, future work must also pay attention to venous valves. It is assumed that these are of great importance for the pDVA procedure. Not only should the change of resistance of a closed venous valve be adequately quantified, but also the opening and closing process of the valve should be included. Any variability in the occurrence of the valves in the foot could also be of interest. Also, the use of a closed-loop model that provides feedback on the hemodynamic changes due to the pDVA procedure is suggested. Finally, it should be mentioned that there is not one general vascular network in the human foot. Future work might therefore consider investigating the effect of vascular network variabilities on the pDVA outcome.

6 References

1 Publishing L. The venous system of the foot: anatomy, physiology, and clinical aspects - Servier - Phlebolymphology. https://www.phlebolymphology.org/the-venous-system-of-the-foot-anatomy-physiology-and-clinical-aspects/. Updated August 28, 2015. Accessed July 12, 2022.

2 Norgren L, Hiatt WR, Dormandy JA, Nehler MR, Harris KA, Fowkes FGR. Inter-Society Consensus for the Management of Peripheral Arterial Disease (TASC II). *J Vasc Surg*. 2007;45 Suppl S:S5-67. doi:10.1016/j.jvs.2006.12.037.

3 Tendera M, Aboyans V, Bartelink M-L, et al. ESC Guidelines on the diagnosis and treatment of peripheral artery diseases. *Eur Heart J*. 2011;32(22):2851-2906. doi:10.1093/eurheartj/ehr211.

4 Criqui MH. Peripheral arterial disease--epidemiological aspects. *Vasc Med*. 2001;6(3 Suppl):3-7. doi:10.1177/1358836X0100600i102.

5 Selvin E, Erlinger TP. Prevalence of and risk factors for peripheral arterial disease in the United States: results from the National Health and Nutrition Examination Survey, 1999-2000. *Circulation*. 2004;110(6):738-743. doi:10.1161/01.CIR.0000137913.26087.F0.

6 Criqui MH, Fronek A, Barrett-Connor E, Klauber MR, Gabriel S, Goodman D. The prevalence of peripheral arterial disease in a defined population. *Circulation*. 1985;71(3):510-515. doi:10.1161/01.CIR.71.3.510.

7 Varu VN, Hogg ME, Kibbe MR. Critical limb ischemia. *J Vasc Surg*. 2010;51(1):230-241. doi:10.1016/j.jvs.2009.08.073.

8 Coats P, Wadsworth R. Marriage of resistance and conduit arteries breeds critical limb ischemia. *Am J Physiol Heart Circ Physiol*. 2005;288(3):H1044-50. doi:10.1152/ajpheart.00773.2004.

9 Ginter E, Simko V. Global prevalence and future of diabetes mellitus. *Adv Exp Med Biol*. 2012;771:35-41. doi:10.1007/978-1-4614-5441-0_5.

10 Rowland DT. Global Population Aging: History and Prospects. In: Uhlenberg P, ed. *International Handbook of Population Aging*. Dordrecht: Springer Netherlands; 2009:37-65.

11 Houlind K, Christensen JK, Jepsen JM. Vein arterialization for lower limb revascularization. *J Cardiovasc Surg (Torino)*. 2016;57(2):266-272. Published December 18, 2015.

12 Katsanos K, Tepe G, Tsetis D, Fanelli F. Standards of practice for superficial femoral and popliteal artery angioplasty and stenting. *Cardiovasc Intervent Radiol*. 2014;37(3):592-603. doi:10.1007/s00270-014-0876-3.

13 Arteries of the leg and foot: Anatomy, pathologies | Kenhub. https://www.kenhub.com/en/library/anatomy/arteries-of-the-leg-and-foot. Updated July 12, 2022. Accessed July 12, 2022.

14 Yadav MK, Mohammed AKM, Puramadathil V, Geetha D, Unni M. Lower extremity arteries. *Cardiovasc Diagn Ther*. 2019;9(Suppl 1):S174-S182. doi:10.21037/cdt.2019.07.08.

15 Wikimedia Commons contributors. File:2129ab Lower Limb Arteries Anterior Posterior.jpg. https://commons.wikimedia.org/w/index.php?title=File:2129ab_Lower_Limb_Arteries_Anterior_Posterior.jpg&oldid=494190516. Updated July 2, 2022UTC. Accessed July 2, 2022UTC.

16 Dorsalis pedis artery: Anatomy, branches, supply | Kenhub. https://www.kenhub.com/en/library/anatomy/dorsalis-pedis-artery. Updated January 12, 2022. Accessed January 12, 2022.

17 Guillot C ST. Anatomy, Bony Pelvis and Lower Limb, Foot Arteries. https://www.ncbi.nlm.nih.gov/books/NBK560912/. Updated 2022 Jul 11.

18 Attinger C, Cooper P, Blume P. Vascular anatomy of the foot and ankle. *Operative Techniques in Plastic and Reconstructive Surgery*. 1997;4(4):183-198. doi:10.1016/S1071-0949(97)80025-X.

19 Themes UF. Reconstruction of Heel and Plantar Defects: Free Flap. https://plasticsurgerykey.com/reconstruction-of-heel-and-plantar-defects-free-flap-2/. Updated November 24, 2019. Accessed July 12, 2022.

20 Ricci S, Moro L, Antonelli Incalzi R. The foot venous system: anatomy, physiology and relevance to clinical practice. *Dermatol Surg*. 2014;40(3):225-233. doi:10.1111/dsu.12381.
21 Veins of the lower limb: Anatomy | Kenhub. https://www.kenhub.com/en/library/anatomy/veins-of-the-lower-limb. Updated July 5, 2022. Accessed July 5, 2022.
22 Sangari SK. Veins of the Lower Limb. In: Tubbs RS, Shoja MM, Loukas M, eds. *Bergman's Comprehensive Encyclopedia of Human Anatomic Variation*: Wiley; 2016:900-909.
23 Meissner MH. Lower extremity venous anatomy. *Semin Intervent Radiol*. 2005;22(3):147-156. doi:10.1055/s-2005-921948.
24 Medical gallery of Blausen Medical 2014. *Wiki J Med*. 2014;1(2). doi:10.15347/wjm/2014.010.
25 Flanders Health Blog. Anatomy Of The Lower Extremity Veins - Varicose Veins. https://www.flandershealth.us/varicose-veins/anatomy-of-the-lower-extremity-veins.html. Updated July 12, 2022. Accessed July 12, 2022.
26 Stoner MC, Calligaro KD, Chaer RA, et al. Reporting standards of the Society for Vascular Surgery for endovascular treatment of chronic lower extremity peripheral artery disease. *J Vasc Surg*. 2016;64(1):e1-e21. doi:10.1016/j.jvs.2016.03.420.
27 Sprengers RW, Teraa M, Moll FL, Wit GA de, van der Graaf Y, Verhaar MC. Quality of life in patients with no-option critical limb ischemia underlines the need for new effective treatment. *J Vasc Surg*. 2010;52(4):843-9, 849.e1. doi:10.1016/j.jvs.2010.04.057.
28 Landry GJ. Functional outcome of critical limb ischemia. *J Vasc Surg*. 2007;45 Suppl A:A141-8. doi:10.1016/j.jvs.2007.02.052.
29 Mangiafico RA, Mangiafico M. Medical treatment of critical limb ischemia: current state and future directions. *Curr Vasc Pharmacol*. 2011;9(6):658-676. doi:10.2174/157016111797484107.
30 Rudofker EW, Hogan SE, Armstrong EJ. Preventing Major Amputations in Patients with Critical Limb Ischemia. *Curr Cardiol Rep*. 2018;20(9):74. doi:10.1007/s11886-018-1019-2.
31 Klaphake S, Leur K de, Mulder PG, et al. Mortality after major amputation in elderly patients with critical limb ischemia. *Clin Interv Aging*. 2017;12:1985-1992. doi:10.2147/CIA.S137570.
32 Columbo JA, Davies L, Kang R, et al. Patient Experience of Recovery After Major Leg Amputation for Arterial Disease. *Vasc Endovascular Surg*. 2018;52(4):262-268. doi:10.1177/1538574418761984.
33 Uccioli L, Meloni M, Izzo V, Giurato L, Merolla S, Gandini R. Critical limb ischemia: current challenges and future prospects. *Vasc Health Risk Manag*. 2018;14:63-74. doi:10.2147/VHRM.S125065.
34 Venous Arterialization for CLI: When, Why, and How? Updated May 14, 2018. https://evtoday.com/articles/2018-may/venous-arterialization-for-cli-when-why-and-how. Accessed January 12, 2022.
35 Migliara B. Totally Percutaneous Deep Foot Vein Arterialization in No-option CLTI Patients Anatomical and Technical Key Points. doi:10.21767/2573-4482.20.05.3.
36 Lu XW, Idu MM, Ubbink DT, Legemate DA. Meta-analysis of the clinical effectiveness of venous arterialization for salvage of critically ischaemic limbs. *Eur J Vasc Endovasc Surg*. 2006;31(5):493-499. doi:10.1016/j.ejvs.2005.12.017.
37 Kum S, Huizing E, Schreve MA, et al. Percutaneous deep venous arterialization in patients with critical limb ischemia. *J Cardiovasc Surg (Torino)*. 2018;59(5). doi:10.23736/S0021-9509.18.10569-6.
38 Huizing E. *Treatment modalities for chronic limb-threatening ischemia: strategies and outcomes*; 2021.
39 Ysa A. Commentary: Percutaneous Venous Arterialization: Should We Contain Our Enthusiasm? *J Endovasc Ther*. 2020;27(4):666-668. doi:10.1177/1526602820923059.
40 Clair DG, Mustapha JA, Shishehbor MH, et al. PROMISE I: Early feasibility study of the LimFlow System for percutaneous deep vein arterialization in no-option chronic limb-threatening ischemia: 12-month results. *J Vasc Surg*. 2021;74(5):1626-1635. doi:10.1016/j.jvs.2021.04.057.

41 Huberts W, Heinen SG, Zonnebeld N, et al. What is needed to make cardiovascular models suitable for clinical decision support? A viewpoint paper. *Journal of Computational Science*. 2018;24:68-84. doi:10.1016/j.jocs.2017.07.006.
42 Müller LO, Toro EF. A global multiscale mathematical model for the human circulation with emphasis on the venous system. *Int J Numer Method Biomed Eng*. 2014;30(7):681-725. doi:10.1002/cnm.2622.
43 Murray CD. The Physiological Principle of Minimum Work: I. The Vascular System and the Cost of Blood Volume. *Proc Natl Acad Sci U S A*. 1926;12(3):207-214. doi:10.1073/pnas.12.3.207.
44 Olufsen MS, Peskin CS, Kim WY, Pedersen EM, Nadim A, Larsen J. Numerical simulation and experimental validation of blood flow in arteries with structured-tree outflow conditions. *Ann Biomed Eng*. 2000;28(11):1281-1299. doi:10.1114/1.1326031.
45 Westerhof N, Stergiopulos N, Noble MI. *Snapshots of Hemodynamics*. Boston, MA: Springer US; 2010.
46 The velocity of pulse wave in man. *Proc. R. Soc. Lond. B.* 1922;93(652):298-306. doi:10.1098/rspb.1922.0022.
47 Alastruey J, Parker K, Peiro J, Sherwin S. Lumped parameter outflow models for 1-D blood flow simulations: Effect on pulse waves and parameter estimation. *Communications in Computational Physics*. 2008;4:317-336.
48 Richard E. Matick. Fundamental Concepts of Transmission Lines Derived from AC Theory. In: *Transmission Lines and Communication Networks: An Introduction to Transmission Lines, High-frequency and High-speed Pulse Characteristics and Applications*: IEEE; 1995:1-24.
49 Waal K de, Kluckow M. Superior vena cava flow: Role, assessment and controversies in the management of perinatal perfusion. *Semin Fetal Neonatal Med*. 2020;25(5):101122. doi:10.1016/j.siny.2020.101122.
50 van der Hout-van der Jagt MB, Oei SG, Bovendeerd PHM. A mathematical model for simulation of early decelerations in the cardiotocogram during labor. *Med Eng Phys*. 2012;34(5):579-589. doi:10.1016/j.medengphy.2011.09.004.
51 Bosiers M, Peeters P, D'Archambeau O, et al. AMS INSIGHT--absorbable metal stent implantation for treatment of below-the-knee critical limb ischemia: 6-month analysis. *Cardiovasc Intervent Radiol*. 2009;32(3):424-435. doi:10.1007/s00270-008-9472-8.
52 Kroon W, Huberts W, Bosboom M, van de Vosse F. A numerical method of reduced complexity for simulating vascular hemodynamics using coupled 0D lumped and 1D wave propagation models. *Comput Math Methods Med*. 2012;2012:156094. doi:10.1155/2012/156094.
53 Bar Massada A, Carmel Y. Incorporating output variance in local sensitivity analysis for stochastic models. *Ecological Modelling*. 2008;213(3-4):463-467. doi:10.1016/j.ecolmodel.2008.01.021.
54 Zareen Ashfaque Khan, Mohammad Afzal Khan, Faris Mohammednouraltaf, Abdullah G Alkhushi, Wardah A Alasmari. Diameter of the Dorsalis Pedis Artery and its Clinical Relevance. *IOSR Journal of Dental and Medical Sciences*. 2016;15:129-133. doi:10.9790/0853-150508129133.
55 Be'eri E, Maier SE, Landzberg MJ, Chung T, Geva T. In vivo evaluation of Fontan pathway flow dynamics by multidimensional phase-velocity magnetic resonance imaging. *Circulation*. 1998;98(25):2873-2882. doi:10.1161/01.CIR.98.25.2873.
56 Cheng CP, Herfkens RJ, Taylor CA. Inferior vena caval hemodynamics quantified in vivo at rest and during cycling exercise using magnetic resonance imaging. *Am J Physiol Heart Circ Physiol*. 2003;284(4):H1161-7. doi:10.1152/ajpheart.00641.2002.
57 Itzchak Y, Modan M, Adar R, Deutsch V. External iliac artery blood flow in patients with arteriosclerosis obliterans. *Am J Roentgenol Radium Ther Nucl Med*. 1975;125(2):437-441. doi:10.2214/ajr.125.2.437.

58 Lewis P, Psaila JV, Davies WT, McCarty K, Woodcock JP. Measurement of volume flow in the human common femoral artery using a duplex ultrasound system. *Ultrasound in Medicine & Biology*. 1986;12(10):777-784. doi:10.1016/0301-5629(86)90075-X.
59 Wolf RL, King BF, Torres VE, Wilson DM, Ehman RL. Measurement of normal renal artery blood flow: cine phase-contrast MR imaging vs clearance of p-aminohippurate. *AJR Am J Roentgenol*. 1993;161(5):995-1002. doi:10.2214/ajr.161.5.8273644.
60 Liang H-L. Doppler Flow Measurement of Lower Extremity Arteries Adjusted by Pulsatility Index. *AJR Am J Roentgenol*. 2020;214(1):10-17. doi:10.2214/AJR.19.21280.
61 Schreve MA, Huizing E, Kum S, Vries J-PPM de, Borst GJ de, Ünlü Ç. Volume Flow and Peak Systolic Velocity of the Arteriovenous Circuit in Patients after Percutaneous Deep Venous Arterialization. *Diagnostics (Basel)*. 2020;10(10). doi:10.3390/diagnostics10100760.
62 Bollinger A, Barras JP, Mahler F. Measurement of foot artery blood pressure by micromanometry in normal subjects and in patients with arterial occlusive disease. *Circulation*. 1976;53(3):506-512. doi:10.1161/01.cir.53.3.506.
63 Ebisudani S. Three-dimensional analysis of the arterial patterns of the lateral plantar region. *Scand J Plast Reconstr Surg Hand Surg*. 2008;42(4):174-181. doi:10.1080/02844310802033927.
64 Macchi V, Tiengo C, Porzionato A, et al. Correlation between the course of the medial plantar artery and the morphology of the abductor hallucis muscle. *Clin Anat*. 2005;18(8):580-588. doi:10.1002/ca.20147.
65 Ozer MA, Govsa F, Bilge O. Anatomic study of the deep plantar arch. *Clin Anat*. 2005;18(6):434-442. doi:10.1002/ca.20126.
66 Whelan JH, Lazoritz JP, Kiser C, Vardaxis V. Location of the Deep Plantar Artery: A Cadaveric Study. *J Am Podiatr Med Assoc*. 2020;110(6). doi:10.7547/18-215.
67 Chepte AP, Ambiye MV. MORPHOMETRIC ANALYSIS OF LATERAL TARSAL ARTERY AND ITS SURGICAL IMPORTANCE. *IJAR*. 2017;5(3.2):4187-4190. doi:10.16965/ijar.2017.281.
68 Hou Z, Zou J, Wang Z, Zhong S. Anatomical classification of the first dorsal metatarsal artery and its clinical application. *Plast Reconstr Surg*. 2013;132(6):1028e-1039e. doi:10.1097/PRS.0b013e3182a97de6.
69 Corley GJ, Broderick BJ, Nestor SM, et al. The anatomy and physiology of the venous foot pump. *Anat Rec (Hoboken)*. 2010;293(3):370-378. doi:10.1002/ar.21085.
70 Binns M, Pho RW. Anatomy of the 'venous foot pump'. *Injury*. 1988;19(6):443-445. doi:10.1016/0020-1383(88)90144-1.

7 Appendix

A

Data tables for arteries and veins

Table 4, Physiological data for arteries and veins based on the work of Müller and Toro. Ref.: reference number, l: length; r_0: inlet radius; r_1: outlet radius; c: wave speed. The calculated compliances of the segments were reduced by 25%.

Ref.	Vessel Name	l [cm]	r_0 [cm]	r_1 [cm]	c [m/s]
1	Ascending aorta	2,00	1,53	1,42	5,11
2	Aortic arch I	3,00	1,42	1,34	5,11
3	Brachiocephalic artery	3,50	0,65	0,62	5,91
4	Right subclavian artery I	3,50	0,43	0,41	5,29
5	Right carotid artery	17,70	0,40	0,37	5,92
7	Right subclavian artery II	39,80	0,41	0,23	5,38
8	Right radius	22,00	0,18	0,14	10,12
9	Right ulnar artery I	6,70	0,22	0,22	8,78
10	Aortic arch II	4,00	1,34	1,25	5,11
11	Left carotid artery	20,80	0,40	0,37	5,92
12	Thoracic aorta I	5,50	1,25	1,12	5,11
13	Thoracic aorta II	10,50	1,12	0,92	5,11
14	Intercostal artery	7,30	0,30	0,30	7,13
15	Left subclavian artery I	3,50	0,43	0,41	5,29
17	Left subclavian artery II	39,80	0,41	0,23	5,38
18	Left ulnar artery I	6,70	0,22	0,22	8,78
19	Left radius	22,00	0,18	0,14	10,12
20	Celiac artery I	2,00	0,35	0,30	5,86
21	Celiac artery II	2,00	0,30	0,25	6,54
22	Hepatic artery	6,50	0,28	0,25	6,86

23	Splenic artery	5,80	0,18	0,15	7,22
24	Gastric artery	5,50	0,20	0,20	6,40
25	Abdominal aorta I	5,30	0,92	0,84	5,11
26	Superior mesenteric artery	5,00	0,40	0,35	5,77
27	Abdominal aorta II	1,50	0,84	0,81	5,11
28	Right renal artery	3,00	0,28	0,28	6,05
29	Abdominal aorta III	1,50	0,81	0,79	5,11
30	Left renal artery	3,00	0,28	0,28	6,05
31	Abdominal aorta IV	12,50	0,79	0,63	5,11
32	Inferior mesenteric artery	3,80	0,20	0,18	6,25
33	Abdominal aorta V	8,00	0,63	0,55	5,11
34	Right common iliac artery	5,80	0,40	0,37	5,50
35	Right external iliac artery	14,50	0,37	0,31	7,05
36	Right internal iliac artery	4,50	0,20	0,20	10,10
37	Right deep femoral artery	11,30	0,20	0,20	7,88
38	Right femoral artery	44,30	0,31	0,28	8,10
41	Right posterior tibial artery	34,40	0,18	0,18	11,98
42	Right anterior tibial artery	32,20	0,25	0,25	9,78
43	Right interosseous artery	7,00	0,10	0,10	15,57
44	Right ulnar artery II	17,00	0,20	0,18	12,53
45	Left ulnar artery II	17,00	0,20	0,18	12,53
46	Left interosseous artery	7,00	0,10	0,10	15,57
49	Left common iliac artery	5,80	0,40	0,37	5,50
50	Left external iliac artery	14,50	0,37	0,31	7,05
51	Left internal iliac artery	4,50	0,20	0,20	10,10
52	Left deep femoral artery	11,30	0,20	0,20	7,88
53	Left femoral artery	44,30	0,31	0,28	8,10
54	Left posterior tibial artery	34,40	0,18	0,18	11,98
55	Left anterior tibial artery	32,20	0,25	0,25	9,78
84	Superior vena cava I	1,50	0,80	0,80	1,00
85	Superior vena cava II	2,00	0,80	0,80	1,00
86	Right brachiocephalic vein	4,00	0,56	0,56	1,36
87	Left brachiocephalic vein	7,50	0,54	0,54	1,41
88	Left subclavian vein I	3,00	0,56	0,56	1,36
89	Right subclavian vein I	3,00	0,56	0,56	1,36
160	Azygos vein I	2,00	0,43	0,43	1,62
171	Right great saphenous vein I	7,50	0,22	0,23	2,10

172	Left great saphenous vein I	7,50	0,22	0,23	2,10
173	Left posterior tibial vein I	17,30	0,15	0,15	2,38
174	Left anterior tibial vein I	16,00	0,15	0,15	2,38
175	Right popliteal vein	19,00	0,34	0,34	1,80
176	Left popliteal vein	19,00	0,34	0,34	1,80
177	Left femoral vein	25,40	0,35	0,35	1,78
178	Right femoral vein	25,40	0,35	0,35	1,78
179	Right deep femoral vein	12,60	0,35	0,35	1,78
180	Left deep femoral vein	12,60	0,35	0,35	1,78
181	Right external iliac vein	14,40	0,50	0,50	1,47
182	Left external iliac vein	14,40	0,50	0,50	1,47
183	Left internal iliac vein	5,00	0,15	0,15	2,38
184	Right internal iliac vein	5,00	0,15	0,15	2,38
185	Right common iliac vein II	2,00	0,58	0,58	1,34
186	Left common iliac vein II	2,00	0,58	0,58	1,34
187	Right radial vein	40,60	0,20	0,20	2,18
188	Left interosseous vein	7,00	0,10	0,10	2,67
189	Right ulnar vein II	30,60	0,20	0,20	2,18
190	Left ulnar vein II	30,60	0,20	0,20	2,18
191	Left interosseous vein	7,00	0,10	0,10	2,67
192	Left radial vein	40,60	0,20	0,20	2,18
193	Left subclavian vein III	27,00	0,52	0,52	1,44
194	Right subclavian vein III	27,00	0,52	0,52	1,44
195	Left subclavian vein II	3,00	0,52	0,52	1,44
196	Right subclavian vein II	3,00	0,52	0,52	1,44
197	Left ulnar vein I	10,00	0,20	0,20	2,18
198	Inferior vena cava I	2,00	0,76	0,76	1,05
199	Hepatic vein	6,80	0,49	0,49	1,50
200	Inferior vena cava II	1,50	0,76	0,76	1,05
201	Inferior vena cava III	1,50	0,76	0,76	1,05
202	Inferior vena cava IV	12,50	0,76	0,76	1,05
203	Inferior vena cava V	8,00	0,76	0,76	1,05
204	Right common iliac vein I	3,80	0,58	0,58	1,34
205	Left common iliac vein I	3,80	0,58	0,58	1,34
206	Right ulnar vein I	10,00	0,20	0,20	2,18
207	Left renal vein	3,20	0,25	0,25	2,03
208	Right renal vein	3,20	0,25	0,25	2,03

209	Ascending lumbar vein	23,00	0,20	0,20	2,18
210	Hemiazygos vein	23,00	0,28	0,28	1,95
211	Inferior mesenteric vein	6,00	0,45	0,45	1,57
212	Right posterior tibial vein I	17,30	0,15	0,15	2,38
213	Right anterior tibial vein I	16,00	0,15	0,15	2,38
216	Right lumbar vein	3,80	0,10	0,10	2,67
217	Left lumbar vein	3,80	0,10	0,10	2,67
242	Right internal jugular vein V	1,00	0,40	0,40	1,67
243	Left internal jugular vein V	1,00	0,62	0,62	1,27
244	Azygos vein II	28,00	0,43	0,43	1,62
245	Inferior vena cava VI	13,30	0,76	0,76	1,05
250	Intercostal vein	2,00	0,40	0,40	1,67
251	Right posterior tibial vein II	17,30	0,15	0,15	2,38
252	Right anterior tibial vein II	16,00	0,15	0,15	2,38
253	Right great saphenous vein II	37,50	0,15	0,19	2,31
254	Left great saphenous vein II	37,50	0,15	0,19	2,31
255	Left anterior tibial vein II	16,00	0,15	0,15	2,38
256	Left posterior tibial vein I	17,30	0,15	0,15	2,38
257	Right great saphenous vein III	30,00	0,19	0,22	2,17
258	Left great saphenous vein III	30,00	0,19	0,22	2,17

Table 5, Estimated physiological data for arteries in the foot. Ref.: reference number, l: length; D_0: inlet diameter; D_1: outlet diameter. References next to values indicate that either measurements, ratios, or other information from literature were used to estimate the value. All diameters at the dorsal side in the model are reduced by 25% (perforators are excluded). Metatarsal perforator diameters are reduced by 70%.

Ref.	Vessel Name	l [mm]	D_0 [mm]	D_1 [mm]	c [m/s]
301	Right lateral plantar arch	78,9[63]	3,2	1,9	11,98
302	Right medial plantar arch	26,5[64]	2,09	2,09	11,98
303	Right deep branch of the medial arch	52,4	1,4[64]	1,4	11,98
304	Right superficial branch of the medial arch	52,4	1,85	1,14	11,98
305	Right deep plantar artery (1. met.)	10,0[65]	1,49[66]	1,49	11,98
318	Right perforating artery (2. met.)	10,0[65]	1,49	1,49	11,98
319	Right perforating artery (3. met.)	10,0[65]	1,04[65]	1,04	11,98
320	Right perforating artery (4. met.)	10,0[65]	1,04[65]	1,04	11,98
306	Right 1. Met. artery	71,0	1,14	1,14	11,98
307	Right 2. met. artery	72,0	1,14	1,14	11,98
308	Right 3. met. artery	68,0	1,14	1,14	11,98
309	Right 4. met. artery	63,0	1,14	1,14	11,98

310	Right fibular plantar superficial artery	68,5	1,14[63]	1,14	11,98
311	Right plantar arch	11,5[65]	1,75	1,75	11,98
312	Right plantar arch	11,5[65]	1,75	1,75	11,98
313	Right plantar arch	11,5[65]	1,75	1,75	11,98
314	Right plantar arch	11,5[65]	1,75	1,75	11,98
316	Right continuation of the superficial branch of med. a.	68,5	1,14[64]	1,14	11,98
401	Left lateral plantar arch	78,9[63]	3,20	1,90	11,98
402	Left medial plantar arch	26,5[64]	2,09	2,09	11,98
403	Left deep branch of the medial arch	52,4	1,40[64]	1,40	11,98
404	Left superficial branch of the medial arch	52,4	1,85	1,14	11,98
405	Left deep plantar artery (1. met.)	10,0[65]	1,49	1,49	11,98
418	Left perforating artery (2. met.)	10,0[65]	1,49	1,49	11,98
419	Left perforating artery (3. met.)	10,0[65]	1,04[65]	1,04	11,98
420	Left perforating artery (4. met.)	10,0[65]	1,04[65]	1,04	11,98
406	Left 1. metatarsal artery	71,0	1,14	1,14	11,98
407	Left 2. met. artery	72,0	1,14	1,14	11,98
408	Left 3. met. artery	68,0	1,14	1,14	11,98
409	Left 4. met. artery	63,0	1,14	1,14	11,98
410	Left fibular plantar superficial artery	68,5	1,14[63]	1,14	11,98
411	Left plantar arch	11,5[65]	1,75	1,75	11,98
412	Left plantar arch	11,5[65]	1,75	1,75	11,98
413	Left plantar arch	11,5[65]	1,75	1,75	11,98
414	Left plantar arch	11,5[65]	1,75	1,75	11,98
416	Left continuation of the superficial branch of med. a.	68,5	1,14[64]	1,14	11,98
501	Right dorsalis pedis	78,9	2,99[54]	2,22[54]	9,78
502	Right lateral tarsal artery	34,1[67]	1,92[67]	1,92	9,78
503	Right arcuate artery	11,5	2,04	2,04	9,78
504	Right arcuate artery	11,5	2,04	2,04	9,78
505	Right arcuate artery	11,5	2,04	2,04	9,78
506	Right arcuate artery	11,5	2,04	2,04	9,78
507	Right 1st dorsal metatarsal a.	62,1[66]	1,34[68]	1,34	9,78
508	Right 2nd dorsal met. a.	62,1	1,34	1,34	9,78
509	Right 3rd dorsal met. a.	62,1	1,34	1,34	9,78
510	Right 4th dorsal met. a.	62,1	1,34	1,34	9,78
511	Right continuation of the lateral tarsal artery	62,1	1,34	1,34	9,78

601	Left dorsalis pedis	78,9	2,99[54]	2,22	9,78
602	Left lateral tarsal artery	34,1[67]	1,92[67]	1,92	9,78
603	Left arcuate artery	11,5	2,04	2,04	9,78
604	Left arcuate artery	11,5	2,04	2,04	9,78
605	Left arcuate artery	11,5	2,04	2,04	9,78
606	Left arcuate artery	11,5	2,04	2,04	9,78
607	Left 1st dorsal metatarsal a.	62,1[66]	1,34[68]	1,34	9,78
608	Left 2nd dorsal met. a.	62,1	1,34	1,34	9,78
609	Left 3rd dorsal met. a.	62,1	1,34	1,34	9,78
610	Left 4th dorsal met. a.	62,1	1,34	1,34	9,78
611	Left continuation of the lateral tarsal artery	62,1	1,34	1,34	9,78

Table 6, Estimated physiological data for veins in the foot. Ref.: reference number, l: length; D_0: inlet diameter; D_1: outlet diameter. References next to geometrical values indicate that information from literature was used for estimation. All diameters at the dorsal side in the model are reduced by 40% and at the plantar side by 20% (perforators are excluded). Metatarsal perforator diameters are reduced by 70%.

Ref.	**Vessel Name**	**l [mm]**	**D_0 [mm]**	**D_1 [mm]**	**c [m/s]**
701	Right plantar arch	9,6[69]	4.40[70]	4.40	2,38
702	Right plantar arch	9,6[69]	4.40[70]	4.40	2,38
703	Right plantar arch	9,6[69]	4.40[70]	4.40	2,38
704	Right plantar arch	9,6[69]	4.40[70]	4.40	2,38
705	Right plantar arch	9,6[69]	4.40[70]	4.40	2,38
706	Right lateral plantar vein	42,0[69]	5,70	5,70	2,38
707	Right medial plantar vein	19,0[69]	3,70	3,70	2,38
708	Right superf. medial branch	70,0	2,10	2,10	2,38
709	Right 1st metatarsal vein	70,0	2,10	2,10	2,38
710	Right 2nd metatarsal vein	70,0	2,10	2,10	2,38
711	Right 3rd metatarsal vein	70,0	2,10	2,10	2,38
712	Right 4th metatarsal vein	70,0	2,10	2,10	2,38
713	Right fibular plantar superfr. branch	70,0	2,10	2,10	2,38
714	Right medial plantar vein	19,0[69]	3,70	3,70	2,38
715	Right lateral plantar vein	42,0[69]	5,70[70]	5,70	2,38
716	Right lateral perforator	10,0	2,00	2,00	2,38
717	Right medial perforator	10,0	2,00	2,00	2,38
801	Left plantar arch	9,6[69]	4,40[70]	4,40	2,38
802	Left plantar arch	9,6[69]	4,40[70]	4,40	2,38
803	Left plantar arch	9,6[69]	4,40[70]	4,40	2,38

804	Left plantar arch	9,6[69]	4,40[70]	4,40	2,38
805	Left plantar arch	9,6[69]	4.40	4,40	2,38
806	Left lateral plantar vein	42,0[69]	5,70	5,70	2,38
807	Left medial plantar vein	19,0[69]	3,70	3,70	2,38
808	Left superf. medial branch	70,0	2,10	2,10	2,38
809	Left 1st metatarsal vein	70,0	2,10	2,10	2,38
810	Left 2nd metatarsal vein	70,0	2,10	2,10	2,38
811	Left 3rd metatarsal vein	70,0	2,10	2,10	2,38
812	Left 4th metatarsal vein	70,0	2,10	2,10	2,38
813	Left fibular plantar superf. branch	70,0	2,10	2,10	2,38
814	Left medial plantar vein	19,0[69]	3,70	3,70	2,38
815	Left lateral plantar vein	42,0[69]	5,70[70]	5,70	2,38
816	Left lateral perforator	10,0	2,00	2,00	2,38
817	Left medial perforator	10,0	2,00	2,00	2,38
901	Right 1. metat. dorsal vein	62,1	2,50	2,50	2,38
902	Right 2. metat. dorsal vein	62,1	2,50	2,50	2,38
903	Right 3. metat. dorsal vein	62,1	2,50	2,50	2,38
904	Right 4. metat. dorsal vein	62,1	2,50	2,50	2,38
905	Right lateral dorsal digital vein of 5th toe	62,1	2,50	2,50	2,38
906	Right dorsal venous arch	11,5	5.10	5.10	2,38
907	Right dorsal venous arch	11,5	5.10	5.10	2,38
908	Right dorsal venous arch	11,5	5.10	5.10	2,38
909	Right dorsal venous arch	11,5	5.10	5.10	2,38
910	Right dorsal vein of the great toe	39,5	5,30	5,30	2,38
911	Right lateral tarsal vein	17,1	3,40	5,80	2,38
912	Right Deep plantar vein 1. met.	10,0	3,70	3,70	2,38
913	Right Deep plantar vein 2. met.	10,0	3,70	3,70	2,38
914	Right Deep plantar vein 3. met.	10,0	2,59	2,59	2,38
915	Right Deep plantar vein 4. met.	10,0	2,59	2,59	2,38
916	Right dorsal vein of the great toe	39,4	5,30	5,30	2,38
917	Right lateral tarsal vein	17,1	3,40	5,80	2,38
1001	Left 1. metat. dorsal vein	62,1	2,50	2,50	2,38
1002	Left 2. metat. dorsal vein	62,1	2,50	2,50	2,38
1003	Left 3. metat. dorsal vein	62,1	2,50	2,50	2,38
1004	Left 4. metat. dorsal vein	62,1	2,50	2,50	2,38
1005	Left lateral dorsal digital vein of 5th toe	62,1	2,50	2,50	2,38

1006	Left dorsal venous arch	11,5	5.10	5.10	2,38
1007	Left dorsal venous arch	11,5	5.10	5.10	2,38
1008	Left dorsal venous arch	11,5	5.10	5.10	2,38
1009	Left dorsal venous arch	11,5	5.10	5.10	2,38
1010	Left dorsal vein of the great toe	39,4	5,30	5,30	2,38
1011	Left lateral tarsal vein	17,1	3,40	5,80	2,38
1012	Left Deep plantar vein 1. met.	10,0	3,70	3,70	2,38
1013	Left Deep plantar vein 2. met.	10,0	3,70	3,70	2,38
1014	Left Deep plantar vein 3. met.	10,0	2,59	2,59	2,38
1015	Left Deep plantar vein 4. met.	10,0	2,59	2,59	2,38
1016	Left dorsal vein of the great toe	39,4	5,30	5,30	2,38
1017	Left lateral tarsal vein	17,1	3,40	5,80	2,38

B

Data tables for the AV-connections

Table 7, Simple AV-connections after Müller and Toro[42]. Note that each connection is divided into three 0D models (arterioles, capillaries, and venules) and one input impedance. Units are C [$\frac{ml}{mmHg}$], R|Z_{inp} [$\frac{mmHg \cdot s}{ml}$] and L [$\frac{mmHg \cdot s^2}{ml}$]. The compliances of the AV-connections in the model are reduced by 25%.

Artery	Vein	Z_{inp}	R_{al}	L_{al}	C_{al}	R_{cp}	L_{cp}	L_{cp}	R_{vn}	L_{vn}	C_{vn}
8	**187**	13,5055	17,0300	0,0180	0,0140	6,5500	0,0029	0,0014	2,1000	0,0052	0,0430
43	**188**	39,4048	393,7000	0,0700	0,0043	151,4000	0,0117	0,0004	48,5000	0,0209	0,0129
44	**189**	9,9182	19,6900	0,0180	0,0140	7,5700	0,0029	0,0014	2,4200	0,0052	0,0430
45	**190**	9,9182	19,6900	0,0180	0,0140	7,5700	0,0029	0,0014	2,4200	0,0052	0,0430
46	**191**	39,4048	393,7000	0,0700	0,0043	151,4000	0,0117	0,0004	48,5000	0,0209	0,0129
19	**192**	13,5055	17,0300	0,0180	0,0140	6,5500	0,0029	0,0014	2,1000	0,0052	0,0430
37	**179**	4,9857	13,3700	0,0140	0,1150	5,1400	0,0023	0,0023	1,6500	0,0042	0,0680
52	**180**	4,9857	13,3700	0,0140	0,1150	5,1400	0,0023	0,0023	1,6500	0,0042	0,0680
36	**184**	6,3903	23,4800	0,0180	0,0182	9,0300	0,0030	0,0014	2,8900	0,0054	0,1080
51	**183**	6,3903	23,4800	0,0180	0,0182	9,0300	0,0030	0,0014	2,8900	0,0054	0,1080
32	**211**	4,8972	30,7400	0,0200	0,0178	11,8500	0,0033	0,0011	3,7800	0,0060	0,0330
28	**208**	2,0247	4,3100	0,0080	0,0680	1,6600	0,0014	0,0067	0,5300	0,0024	0,2000
30	**207**	2,0247	4,3100	0,0080	0,0680	1,6600	0,0014	0,0067	0,5300	0,0024	0,2000
14	**250**	2,0050	5,6100	0,0090	0,1390	2,1600	0,0015	0,0139	0,6900	0,0027	0,4170

Table 8, Values for complex AV-connections after Müller and Toro[42]. Units are C [$\frac{ml}{mmHg}$], R|Z_{inp} [$\frac{mmHg \cdot s}{ml}$] and L [$\frac{mmHg \cdot s^2}{ml}$]. The compliances of the AV-connection in the model are reduced by 25%.

Vessel	Z_{inp}	R_{al}	L_{al}	C_{al}	R_{al}	L_{cp}	C_{cp}	R_{vn}	L_{vn}	C_{vn}
22	2,7594	16,24	0,015	0,021	6,24	0,0024	0,0021	-	-	-
26	1,1634	3,85	0,007	0,081	1,48	0,0012	0,0081	-	-	-
23	7,8931	21,33	0,018	0,014	8,2	0,003	0,0014	-	-	-
24	4,0493	8,91	0,012	0,033	3,43	0,0019	0,0032	-	-	-
199	-	-	-	-	-	-	-	0,255	0,0013	0,527

Table 9, Estimated values for pedal AV-connections. Units are C [$\frac{ml}{mmHg}$], R|Z_{inp} [$\frac{mmHg \cdot s}{ml}$] and L [$\frac{mmHg \cdot s^2}{ml}$].

Artery	Vein	Z_{inp}	C	R	L
310	**713**	106,995	0,014	334,806	0,184
309	**712**	106,995	0,014	334,806	0,184
308	**711**	106,995	0,014	334,806	0,184
307	**710**	106,995	0,014	334,806	0,184
306	**709**	106,995	0,014	334,806	0,184
316	**708**	106,995	0,014	334,806	0,184
507	**901**	112,389	0,059	200,962	0,164
508	**902**	112,389	0,059	200,962	0,164
509	**903**	112,389	0,059	200,962	0,164
510	**904**	112,389	0,059	200,962	0,164
511	**905**	112,389	0,059	200,962	0,164
410	**813**	106,995	0,014	334,806	0,184
409	**812**	106,995	0,014	334,806	0,184
408	**811**	106,995	0,014	334,806	0,184
407	**810**	106,995	0,014	334,806	0,184
406	**809**	106,995	0,014	334,806	0,184
416	**808**	106,995	0,014	334,806	0,184
607	**1001**	112,389	0,059	200,962	0,164
608	**1002**	112,389	0,059	200,962	0,164
609	**1003**	112,389	0,059	200,962	0,164
610	**1004**	112,389	0,059	200,962	0,164
611	**1005**	112,389	0,059	200,962	0,164